Published in final edited form as:
Adv Drug Deliv Rev. 2012 October ; 64(13): 1488–1507. doi:10.1016/j.addr.2012.07.008.

Personalized nanomedicine advancements for stem cell tracking☆

Mirek Janowski[a,b,c,d], **Jeff W.M. Bulte**[a,b,e,f,g], and **Piotr Walczak**[a,b,*]

[a]Russell H. Morgan Department of Radiology and Radiological Science, Division of MR Research, The Johns Hopkins University School of Medicine, Baltimore, MD 21205, USA [b]Cellular Imaging Section and Vascular Biology Program, Institute for Cell Engineering, The Johns Hopkins University School of Medicine, Baltimore, MD 21205, USA [c]NeuroRepair Department, Mossakowski Medical Research Centre, Polish Academy of Sciences, Warsaw 02-106, Poland [d]Department of Neurosurgery, Mossakowski Medical Research Centre, Polish Academy of Sciences, Warsaw 01-809, Poland [e]Department of Chemical and Biomolecular Engineering, The Johns Hopkins University Whiting School of Engineering Baltimore, MD 21205, USA [f]Department of Biomedical Engineering, The Johns Hopkins University School of Medicine, Baltimore, MD 21205, USA [g]Department of Oncology, The Johns Hopkins University School of Medicine, Baltimore, MD 21205, USA

Abstract

Recent technological developments in biomedicine have facilitated the generation of data on the anatomical, physiological and molecular level for individual patients and thus introduces opportunity for therapy to be personalized in an unprecedented fashion. Generation of patient-specific stem cells exemplifies the efforts toward this new approach. Cell-based therapy is a highly promising treatment paradigm; however, due to the lack of consistent and unbiased data about the fate of stem cells in vivo, interpretation of therapeutic remains challenging hampering the progress in this field. The advent of nanotechnology with a wide palette of inorganic and organic nanostructures has expanded the arsenal of methods for tracking transplanted stem cells. The diversity of nanomaterials has revolutionized personalized nanomedicine and enables individualized tailoring of stem cell labeling materials for the specific needs of each patient. The successful implementation of stem cell tracking will likely be a significant driving force that will contribute to the further development of nanotheranostics. The purpose of this review is to emphasize the role of cell tracking using currently available nanoparticles.

Keywords

Nanoparticles; Transplantation; Stem cells; Imaging; Theranostics

1. Why do we need Personalized Medicine?

The practice of medicine represents a unique relationship between the health professional and the patient [1–3]. Thus, a personalized approach has always been the essence of health

☆This review is part of the *Advanced Drug Delivery Reviews* theme issue on “Personalized nanomedicine”.

*Corresponding author at: The Russell H. Morgan Department of Radiology and Radiological Science, Division of MR Research, Institute for Cell Engineering, Johns Hopkins University School of Medicine, Broadway Research Building Rm 649, 733 N Broadway, Baltimore, MD 21205, USA. pwalczak@mri.jhu.edu. .

care delivery. The patient's demographics, family history, the results of blood and radiological exams and of biopsies have been employed for years to tailor a specific therapy for each patient. That is why the personalized aspect of medicine is continuously being emphasized, and has recently gained more and more interest.

The term "Personalized Medicine" has recently acquired a new dimension as a result of the explosion of data about biomedical processes. Anatomical and physiological data on a molecular level can now be generated for each individual patient. It has long been anticipated that biotechnology will revolutionize the medicine of the future [4]. We live at a time when this is becoming a reality. Indeed, the term "Personalized Medicine" was coined because of the advances in clinical pharmacogenetics [5–7] and was popularized by Hood, a visionary doctor and researcher, who invented the DNA and protein sequencer and synthesizer [8]. Hood developed the concept of "4×P" medicine, which is short for "Predictive, Preventive, Personalized, and Participatory medicine" [9]. However, such a novel concept, based on using the entire breadth of data available about each patient to make therapy more individualized, clashed with the current classical approach of evidence-based medicine (EBM) [10]. EBM focuses on using the best evidence from randomized clinical trials (RCTs) about treatment efficacy. This process requires dichotomization of patients into experimental and control groups, resulting in large heterogeneity within groups [11]. However, RCTs remain the mainstream approach and, as of today, from a legal point of view, they are mandatory to obtain Food and Drug Administration approval for the marketing of therapeutic products [12]. One criticism of RCTs is that a selected pool of "ideal" patients is recruited, which ignores complex clinical situations. As a result, the outcomes of RCTs are relevant to only a fraction of the patient population [13]. Increasing discontent with EBM is leading to growing support for the concept of personalized medicine [14]. As a compromise between the two trends, the new term "personalized EBM," has recently been coined [15].

Whatever the approach, it would seem that personalized medicine will be a definite factor in the practice of medicine, and we must choose to use it wisely to save lives and improve the quality of life for individual patients. The current developments in biotechnology provide us with an unprecedented opportunity to practice personalized medicine in the most effective way. Thus, it is our obligation to develop approaches that meet the current demands of clinical practice and to use personalized medicine to improve the treatment of all patients [16].

2. The stem cell revolution

Although personalized medicine arose from pharmacogenetics [17], it has now infiltrated many fields of healthcare [18–20]. Despite the advances in pharmacology, it became apparent that many disorders were beyond the capabilities of current treatment methods [21]. As a response to widely unmet clinical needs, an approach based on using cells for therapy has emerged [22,23]. The discovery and characterization of stem cells, with self-renewal and differentiation capacities, also accelerated this field, making regenerative medicine a new independent discipline [24]. However, embryonic stem cells are plagued by ethical and immunorejection problems, and a shortage of adult stem cells precludes their wide clinical application. Only the recent discovery of induced pluripotent stem cell technology, which enables any cell of the body (including skin fibroblasts) to be changed into a pluripotent stem cell, with the potential to differentiate toward any cell type in unlimited quantities, may make the advent of large-scale cytotherapeutics possible [25]. Of 106 ongoing and planned neuro-restorative clinical trials, nearly two-thirds focus on cell-based therapy [26]. The possibility to derive, repair, propagate, and transplant cells

specifically for each individual patient takes personalized medicine to an entirely new dimension [27].

A Swedish group, who pioneered cell-based therapy for Parkinson's disease in their proof-of-concept clinical neurotransplantation trials, carefully selected and treated individual patients, thus highlighting the importance of a personalized approach [23,28,29]. However, traditional RCTs later performed in the USA failed to reveal a statistically significant positive effect of cell therapy for Parkinson's disease. Although there were positive effects in some patients, other patients experienced side effects that exacerbated the disease [30,31]. Thus, the EBM approach, which neglects the heterogeneity of response to treatment within groups, may be too simplistic an approach for use with stem cell therapy. The personalized approach, however, seems more likely to succeed with the use of stem cell treatments.

Bone marrow reconstitution by stem cells is a well-established therapy for malignancies [32,33] and aplasias [34,35], and these are excellent examples of the success and impact that cell-based therapy has had on medicine. In contrast, the treatment of diseases that affect many other organs and tissues with stem cell therapy is still in its infancy and requires further development [36]. New technology, such as non-invasive imaging of transplanted cells to monitor their fate in vivo, will be instrumental in developing effective clinical applications for cell therapy [37,38].

There is a wide array of diseases awaiting effective treatment, with neurological disorders being a prominent example of cases where treatment options are scarce, and stem cell-based therapies offer hope for scores of patients. The inconvenience of life-long injections for the treatment of diabetes with inevitable, long-term complications makes diabetes another application where cell replacement therapy is very attractive, especially in the light of the increasing incidence of this disease [39]. Stem cell therapy for diabetes and liver failure with cadaver-derived cells resulted in some positive effects [40]; however, limited access to those sources precludes widespread clinical application [41]. The effective production of hepatocytes from induced pluripotent stem cells (iPSC) [42] and from embryonic stem cells (ESC) [43,44] has been reported, and that may address the problem of donor material shortage. In addition to the hepatocyte replacement approach, the administration of bone marrow stem cells enhanced the functional hepatic reserve after extended hepatectomy [45]. It has also been shown that transplanted bone marrow cells may counteract the complications of anti-cancer therapy by restoring long-term fertility [46] and helping to repair the intestinal mucosa [47]. Connective tissue diseases, including disc and joint disorders, occur frequently in young adults, causing long-term absence from work, and forcing premature retirement, and, as a consequence, major socio-economic challenges [48,49]. The positive effects of cell therapy for musculoskeletal injuries were demonstrated initially in race-horses [50,51]. This was followed by the spectacular therapeutic success in Bartolo Colon, a New York Yankee baseball pitcher who suffered from a shoulder injury, but who could return to this sport after stem cell therapy (May 14 2011, The Wall Street Journal). There has also been extraordinary progress in the use of stem cells for the ex vivo production of connective tissue structures, such as the trachea, and subsequent successful transplantation in patients [52].

Stem cell-based therapy is very promising for many disorders, with some encouraging outcomes already reported. However, the results are still variable, making the likelihood quite low that insurance companies and national health systems will cover such procedures, at least in the nearest future.

3. Living in the nanoworld

The tremendous progress in material science and biotechnology has enabled unparalleled miniaturization and manipulation of materials at the molecular or even atomic scale. By definition, a nanotechnology deals with materials that range from 1 to 100 nm in size in at least one of three dimensions. Fabrication at the nanoscale level fundamentally multiplies the repertoire of attainable products and offers products of unprecedented properties. There are two main approaches to nanofabrication: top-down and bottom-up [53].

The top-down approach is based on using nano-machine tools to shape matter. This lies within the domain of physicists, and one of the most spectacular examples was the weaving of a pattern from single atoms using atomic force microscopy (AFM) [54]. This type of nanofabrication has also found its way to surgery with the concept of nanosurgery using multi-photon microscopy [55].

The bottom-up approach is based on the self-assembly of atoms or molecules toward nanostructures [56]. In other words, the principle of this approach is to make a non-covalent bond art out of covalently bond blocks. Although this concept seems new, it has already been employed in nature, with the most apparent manifestation that of complex protein structures self-organizing from a simple amino-acid sequence. This type of nanofabrication is now being widely investigated, primarily by chemists, to create functional, highly ordered, hierarchical structures. There is a wide diversity of self-organizing structures:

– Helical strands—It was shown that enzymatically synthesized phospholipid-nucleoside conjugates spontaneously form helical strands with a diameter of 5 nm, as in the case of nucleic acids [57].

– Nanoparticles—Proteins [58], lipids [59], and alcohols [60] self-assembled in the presence of nano-sized iron oxide particles.

– Nanocoatings (exo-scaffolds)—Synthetic [61] and natural [62] polymers have been found to coat single cells with nanometric layers.

– Nanogels—Crosslinking polymers have yielded nanometer-sized gels [63].

– Nanofibers—Molecules that self-assemble in nanofibers (which were found to promote wound healing [64] or could be used as a scaffold for tissue engineering [65]).

– Nanospheres/nanobubbles—Native RNA was converted into stable RNA nanospheres by ultrasonic waves. Such spheres may then be inserted into cells [66].

The techniques for fabrication, with atomic precision, continue to increase; thus, further advances toward high-throughput manufacturing are on the horizon. The above-listed nanostructures have found numerous applications in virtually all fields of science and medicine, and also proved to be well-suited for stem cell labeling and non-invasive, in vivo tracking of stem cells.

4. Stem cell tracking and personalized nanomedicine

The diversity of nanomaterials that have recently become available opens the opportunity to tailor these materials to the specific needs of individual patients [67]. While the proof-of-principle of personalized nanomedicine has been reported, applying these novel tools clinically is not trivial [68]. Adding stem cells to this equation makes things even more complex [69]. Introducing cell-based therapy as a new potent strategy in the therapeutic arsenal has been met with great enthusiasm, but putting this therapy into routine clinical practice proved difficult. Studies about the transplantation of stem cells of various origins have been conducted for years, initially in animal models and then in patients, offering hope

for effective treatment. However, there are severe problems with the interpretation of the outcomes of stem cell-based treatments. One of the leading obstacles is the lack of consistent and unbiased data about stem cell distribution and survival in vivo. Typically, for drug development, the pharmacokinetics and pharmacodynamics are routinely employed to characterize the basic features of the tested drugs in the organism [70]. The benefits of any surgical intervention are usually confirmed through post-operative imaging. These methods offer a conclusive assessment and allow a judgment about the efficacy of pharmacotherapy or surgery. Such standards, unfortunately, have not yet been developed for stem cell therapy. Although neuroimaging was strongly supported as a base for rational stem cell therapy [71], to date, only a few clinical studies have followed this recommendation [72]. The resistance to the implementation of cellular imaging into clinical protocols may stem from the notion that transplanted stem cells will undergo self-guidance in terms of their migration and functional integration, which is unrealistic at best, or may be due to the lack of robust, versatile, and validated methods by which to monitor the fate of transplanted stem cells.

Nanotechnology now offers many solutions for labeling cells and those are well-suited for personalized medicine. With cellular imaging, cell transplantation-based therapy may be tailored to the individual patient rather than to a large heterogeneous population. Such an approach, which would consider the pathology of each specific patient, would help to maximize the therapeutic effect. While cell therapy for internal disorders, such as diabetes, liver failure, or myocardial infarction, can be evaluated with more objective measures, neurological disorders are the most challenging in this regard. Although a meta-analysis of preclinical results revealed the positive effects of cell therapy in neurological disorders [73], there is still no consensus about the mechanisms that mediate cell-dependent effects, or about timing, dosage, type of cells, and other factors [74]. Thus, stem cell tracking is expected to play a pivotal role in defining these mechanisms, and this is essential for further optimization of cell therapy [75].

5. Customizing stem cell imaging modalities for specific clinical scenarios

There are many imaging modalities used in clinical practice and the choice of a modality is determined by the specific diagnostic question, availability, and cost-effectiveness. Additional factors that determine the suitability of an imaging method are specificity, sensitivity, resolution, and radiation exposure of individual modalities. Imaging plays a critical and constantly growing role in medicine and there are well-developed imaging algorithms that are routinely used to evaluate the course of many diseases. Consequently, it is of the utmost importance that a new imaging methodology, such as cell tracking, does not interfere with some of the existing critical imaging algorithms. The goal is not only to see transplanted cells, but also to image pathological processes within the organ of interest. Some of the available cellular imaging techniques do interfere with anatomical or functional imaging, such as in the case of iron oxide in MRI. Thus, the selection of an imaging modality should be driven by the need for a particular anatomical or functional imaging technique required for evaluation of the underlying pathology. This concept is termed the “imaging window,” and could be different in each patient, given existing co-morbidities and other factors.

5.1. MRI

Magnetic resonance imaging is capable of producing images of the human body with an unsurpassed detail. It has also been shown, with iron oxide as a cell label, that MRI is an excellent method for detailed demonstration of the cell location after transplantation. In one reported study in cancer patients, iron oxide-labeled cells were injected into lymph nodes, and imaging showed a striking mis-injection rate, with off-target delivery in half the cases [76]. Due to the superior homogeneity of the magnetic field within the brain, MRI has also

been successfully used for neurotransplantation [77]; however, it was shown that iron oxide may interfere with MR imaging parameters [78]. Since various MR imaging techniques, such as functional MRI (fMRI), diffusion tensor imaging (DTI), or perfusion MRI, may be necessary to evaluate the progression of central nervous system (CNS) diseases or the healing process, alternative tracers, including those suitable for other imaging modalities, are desirable. While there is an effort to develop new generation "switch-able" MRI contrast agents, their sensitivity is still below clinical utility [79]. Nevertheless, for many cell therapy applications, especially in cases when a precise reference to anatomy is critical, MRI of iron oxide-labeled cells is still the method of choice.

5.2. X-ray computed tomography (CT)

X-ray CT is characterized by excellent temporal resolution, very high spatial resolution, and satisfactory anatomical and topographical depiction with relatively low soft tissue contrast. As such, it is a potentially interesting candidate modality for stem cell imaging, particularly for applications in the brain or lungs. Well-developed methods for image co-registration [80] enable spatial superposition of images acquired using CT and MRI, and allow complementary multimodality imaging. CT is the leading modality for the evaluation of bone damage and repair[81,82], thus it would be desirable to follow the transplanted cells for bone healing with a different modality so as not to interfere with the CT evaluation of osteogenesis. Compared to MRI, stem cell tracking with CT is far less developed. However, it has been shown that gold nanoparticles can be used to image a molecular target [83] and/or cells [84] in vivo. Labeling of mesenchymal stem cells with gold nanotracers was found to be safe, with no detrimental effects on cell function [85]. In addition to standard X-ray CT scans, it has recently been reported that this modality can produce multi-color images [86,87] that potentially could be used to monitor several different processes simultaneously, including tracking two populations of cells.

5.3. Nuclear medicine

Nuclear medicine is characterized by an excellent in vivo sensitivity and whole-body imaging capabilities. However, the "hot spot" imaging of radionuclides usually requires additional scanning with another anatomy-providing imaging modality, followed by image co-registration and superimposition. Luckily, integrated PET/CT scanners are now widely available. In addition, co-registration of MRI and CT is well-established and those images can readily be fused with PET results [88]. Integrated PET/MRI scanners are another option. The integration of PET and high-field scanners is a major challenge, as this result in interference, with a decreased quality of images in both modalities [89]. Although there has been significant progress in the development of hardware for the purposes of nuclear medicine, the applicability of radionuclide-based cell tracking is still unclear, primarily due to the issues of safety and toxicity. While systemic injection of radionuclides results in negligible whole-body radiation, the situation is quite different for cell labeling. A relatively high accumulation of radionuclides in single-labeled cells and the prolonged (days/weeks) irradiation that concentrates most of the energy within the same cell may be detrimental to stem cells [90]. The superb signal-to-noise ratio may warrant labeling only a fraction of the transplanted cells, but even those can be at risk of mutation and subsequent tumorigenic transformation. Thus, radionuclide-based stem cell tracking in patients should be introduced cautiously. Another limitation of this modality is the short half-life of radioactive tracers, which do not extend one week, even with the longest-lived isotopes. While the clinical application of nuclear medicine for stem cell tracking seems problematic, the application of this modality in the preclinical setting may still be valuable.

5.4. Ultrasonography (USG)

The major advantages of USG are the low cost, wide availability, and lack of toxicity. USG may be easily employed to monitor and navigate the device used for cell injection [91], but visualization of the cells themselves is complex. As in other modalities, transplanted cells require labeling with a contrast agent. A typically used and commercially available contrast agent for USG consists of air bubbles. Functionalized bubbles, injected intravenously, have been used to detect subcutaneously transplanted cells [92]. The bubbles have been found to be taken up by tumor cells, improving tumor visualization with USG [93]. However, the major limitation of USG is associated with the severe attenuation of ultrasound waves by bones, which practically eliminates USG as a robust method for cell tracking within the CNS.

5.5. Optical imaging

Due to light scattering and absorption by the tissues, most applications for optical imaging are in small animals, where bioluminescence imaging, in particular, is intensively exploited to monitor the status of transplanted cells [94–96]. The clinical application of optical imaging, for obvious reasons, is largely limited to superficial targets. One very important application for this approach is based on fluorescent probes that target tumor cells used to guide brain tumor resection in patients. Relatively good tissue penetration by photons in the near infrared wavelength region makes optical probes of these characteristics most promising for broader applications in patients. The so-called “optical window” that offers good tissue penetration is limited by water absorption of the photons above 1300 nm, and hemoglobin absorption below 700 nm [97]. Currently, near-infrared (NIR) spectroscopy is widely used in studies of brain oxygenation [98] or even for fMRI-like assessment of resting-state functional connectivity in the brain [99]. The low cost and portability of near infrared (NIR) scanners contributes to the rapidly growing interest in this modality[100]. Recent advances in nanocrystal formation, with exceptionally high photoluminescence within a near infrared range, have been shown to be very promising in small animal experiments, and may also find applications in the clinical setting [101].

6. Goals of stem cell tracking

Stem cell tracking has been introduced as a response to the need to address distinct scientific questions, including the evaluation of cell distribution, cell survival, and cell function. Stem cell tracking is being applied in a variety of disorders and with many different transplantation routes [102].

6.1. Monitoring cell distribution

The evaluation of cell distribution following transplantation seems to be an essential, basic task, and such as pharmacokinetics for drug development should be recommended for any cell therapy-based study. Determining the location of transplanted cells within the recipients’ body is critically important, and the value of this information increases the farther the distance between the site of the cell deposit and the desired cell destination. The evaluation of cell distribution is usually most important within the first few days after transplantation, and until cells reach the final destination [103,104]. However, in some circumstances, cells may migrate over longer periods of time [105–107]. The intravenous route for cell delivery, with a high degree of uncertainty about cell distribution, is especially appealing for cell tracking [108–111]. The intra-arterial route is more targeted in terms of cell delivery[112], it also can suffer from mis-injection, which, however, can be easily captured by in vivo cell tracking (Fig. 1) [113]. This approach also provides information about the dynamics of cell redistribution or with-in the body. In animals, cell distribution can also be assessed by labor-intensive post-mortem histopathology, but this is not an option

in the clinical setting. Monitoring the time course of cell delivery allows an evaluation of the desired and actual cell locations. With access to that information, the interpretation of experimental/clinical data is much easier. As shown in reports on cell-based therapy trials, the response to cell therapy is often variable, and that variability may, at least in part, result from less than optimal cell delivery in some patients [76]. The response to therapy may also reveal that cell distribution is inadequate or insufficient, and this may account for a suboptimal outcome. In this context, all aspects of cell delivery and cell distribution must be carefully addressed to maximize the chance for optimal cell delivery to the correct destination.

An appropriate assessment of cell distribution requires the application of a high-resolution, tomographic modality, such as MRI, or, alternatively, a multimodality approach that can co-register high-sensitivity low-resolution and low-sensitivity high-resolution acquisitions (i.e., PET and MRI) [114].

6.2. Monitoring cell survival

It has been shown recently that cell tracers used for non-invasive imaging may persist in tissues following cell death [96], or these tracers can be diluted by cellular proliferation [115]. Thus, monitoring cell viability is a more challenging task than was thought originally [116]. In small animals, reporter gene-based (bioluminescence) imaging has been found to be extremely useful, but, as mentioned above, it is not clinically applicable [117], and, as of now, no clinically applicable solution has been found by which to monitor cell viability.

There have been continuous efforts to establish a gene reporter system for MRI and several initial prototype genes have been developed[118,119], but current approaches are still plagued by insufficient sensitivity and specificity [120]. An alternative to reporter genes would be a “smart probe,” producing contrast based on cell viability status. Most desirable probe would be one that produces positive signal within living cells and no signal upon a cell death.

6.3. Monitoring cell function

Direct imaging of the function of cells in vivo can, at present, only be done using quite invasive approaches, such as two-photon microscopy[121]. Non-invasive imaging techniques still lack the sensitivity and resolution to directly image cell function. However, indirect imaging of transplanted cell function has long been used [122,123] to obtain information about cell function. A good example of such indirect monitoring is related to a very specific situation in Parkinson’s disease, where well-defined dopaminergic transmission is compromised by the disease process, and probes targeted to the dopaminergic machinery can visualize its function. While such a functional imaging paradigm has been used to evaluate the efficacy of cell-based therapy, it is not capable of providing a definitive answer about whether recorded dopaminergic transmission stems directly from the transplanted cells, or indirectly, from endogenous repair mechanisms. Nevertheless, indirect measures of grafted cell functionality are an important guide to enable accurate judgments about graft functionality and facilitate further optimization of the therapeutic protocol.

7. Stem cell labels and tracers

The field of stem cell research benefits greatly from nanotechnology, which offers many solutions for stem cell tracking. Nanotechnology provides a variety of direct stem cell labeling options, as well as facilitates the use of other important methods, such as reporter genes. Stem cell tracking techniques can be divided, based on the placement of contrast material, into intracellular, with contrast agent localized within the cell, and extracellular,

where signal is derived from the out-side of a cell, but is closely related to the cell. Stem cell tracers may be detectable by just one modality (unimodal) or by several modalities (multimodal).

7.1. Intracellular labels and tracers

7.1.1. Direct stem cell labels and tracers

7.1.1.1. Unimodal labels and tracers

7.1.1.1.1. Iron oxide nanoparticles: Internalization of iron oxide particles by specific cell populations was observed as early as 80 years ago and was used for the magnetic selection of Kupffer cells [124]. After the introduction of MRI to the clinic, it was reported that facial cosmetics used for mascaras and tattooing resulted in artifacts on MR images, and iron oxide particles were found to be responsible for this effect[125–127]. After coating by polymers to increase biocompatibility and protect aggregation [128], iron oxide particles were used for MR imaging of the liver to diagnose malignancy [129]. There is now a variety of sizes of iron oxide particles available for cell labeling, ranging from micron-sized [130] to nanometer-sized particles [131]. Iron oxide nanoparticles are one of the most frequently used agents for cell tracking.

The first application of iron oxide nanoparticles to label cells other than Kupffer macrophages was the ex vivo labeling of peripheral blood mononuclear cells [132]. That was followed by studies on the labeling and imaging of transplanted neural cells [133–136]. Of note is the fact that the size of iron oxide nanoparticles determines the efficiency of cell up-take, with much higher labeling efficiency for small nanoparticles ca. 70 nm diameter (SPIO), than for ultra-small iron oxide nanoparticles (USPIO) [137]. One of the SPIO formulations (Feridex®) approved by the Food and Drug Administration (FDA) in 1996 as a liver contrast agent, following the development of methods that facilitated the labeling of non-phagocytes, including stem cells, was extensively used and characterized in preclinical research, with the intention to use Feridex® clinically thereafter [138–140]. Unfortunately, in 2008, the company stopped manufacturing Feridex®, citing economic among other reasons, and leaving the field without a clinically approved SPIO agent. Recently Feraheme®, a new formulation of iron oxide, has been approved by the FDA for the treatment of anemia. Due to their ultra-small size (USPIO), labeling cells with these nanoparticles is more challenging; however, recent reports demonstrated a labeling technique for Feraheme® that makes them detectable by MRI [141,142]. A follow-up study demonstrated improved labeling with the use of self-assembling nanocomplexes by combining Feraheme®, heparin, and protamine, yielding larger, ca. 100 nm-size complexes (Fig. 2), facilitating stem cell up-take [143]. Of note is that all these agents are FDA-approved for other clinical uses.

Due to the very strong MRI signal, iron oxide enables almost microscopic visualization of cells, especially when imaged using a high-field MR scanner. However, long-term observation has revealed that SPIO within the tissue and contrast on MRI persists despite the death of transplanted stem cells [96,144,145]. In this context, SPIOs offer robust and specific information about the distribution of labeled cells; however, long-term monitoring of the fate of stem cells requires cautious interpretation. For applications in peripheral organs, dual-modality MRI/PET is an attractive option with SPIO-based MRI reporting on the detailed location of cells and PET imaging of thymidine kinase products reporting on cell viability [146]. Such a strategy for imaging within the CNS is, however, complicated by the lack of penetration of certain PET probes across the blood-brain barrier.

Amid the reported limitations of iron oxide nanoparticles, there have been continued efforts to improve the properties of these agents with a multitude of new surface modifications/

coatings, revealing better labeling and toxicity profiles. Poly(N,N-dimethylacrylamide)-coated maghemite [147], aminosilane coating [148], amine surface modification [149], carboxymethyl chitosan modification [150], 1-hydroxyethylidene-1.1-bisphosphonic acid (HEDP) coating [151], non-toxic protein transduction domain (PTD) conjugation [152], higher density carboxyl groups modification [153], and D-mannose-modification [154] were used for this purpose. The versatile and tunable coating strategies for iron oxide nanoparticles [155], may enhance the customization of labeling for individual applications and the requirements of individual patients.

It has been shown that the contrast mechanism of iron oxide nanoparticles in MRI depends on the particle size. While SPIOs were traditionally used to provide negative T2 contrast, the ultra-small iron oxide nanoparticles, in addition to the T2 contrast, can also produce the more-desirable positive T1 contrast [156]. The large-scale synthesis of uniform and extremely small-sized iron oxide nanoparticles (ESION) for positive T1 contrast may increase the utility of iron oxide as a contrast agent [157].

Another use for iron oxide nanoparticles, beyond providing out-standing MR contrast, is based on their magnetic characteristics that enable the guidance and navigation of labeled cells after transplantation. This can be accomplished with the use of external magnets placed over the target organ, which results in increased stem cell homing to desired organs [158–160].

7.1.1.1.2. Gadolinium nanoparticles: Gadolinium (Gd) is a T1 contrast agent that generates positive contrast, thus avoiding difficulties in the interpretation of signal voids, which often complicate imaging with SPIOs [161]. However, clinically used gadolinium chelates do not produce a positive T1 signal after internalization by the cells [162]. The widespread use of gadolinium as a cell labeling agent may be hampered by difficulties in the synthesis of stable, water soluble solutions [163]. However, recently, there have been several reports on new approaches that incorporate gadolinium within the metal-based core of nanoparticles [164], or polymer-based scaffolds [165]. While Gd chelates are characterized by a relatively low signal per molecule, the formation of gadolinium oxide nanoparticles with certain magnetic properties has been shown to be useful for tracking hematopoietic cells [166]. With the advent of commercially available dextran-coated gadolinium oxide nanoparticles—e.g. Gado CELLTrack (BioPAL)—it is expected that this approach may be further pursued [167]. Further work to optimize the surface coatings of gadolinium oxide nanoparticles is under way, with a range of modifications, such as using shells made of PEG [168] and DEG[169], silica [170], and albumins [171]. Another approach is to capture gadolinium atoms within carbon cages made of nanotubes[172] or fullerenes [173]. However, the cardinal issue that would determine the advantage of gadolinium-based nanoparticles over SPIOs is their clearance after the death of grafted cells. Recently, it has been reported that a free Dex-DOTA-Gd3+ contrast agent clears from the transplantation site, as opposed to iron oxide particles; however, the credibility of this result would have been significantly improved by the presentation of raw MR images and not merely volume-rendered scans, as presented in this publication [174]. Most importantly, prolonged retention of gadolinium will results in release of free Gd^{3+} ions, which are toxic. Hence, it is very unlikely that Gd-based cell tracking will reach the clinic.

7.1.1.1.3. Manganese oxide nanoparticles: The similarity of manganese and gadolinium, with regard to providing T1 contrast in MRI, has been reported some time ago [175]. However, the in vivo [176,177] and in vitro [178] neurotoxicity of manganese favored gadolinium as a widely clinically applicable contrast agent [179]. Notably, it has been recently reported that the toxicity of manganese to cells other than neurons is low, comparable to that of iron, and much lower than that of silver and molybdenum oxide [180].

An efficient method for the production of manganese oxide nanoparticles, followed by coating with a biocompatible PEG-phospholipid shell, sparked interest in manganese as an MRI contrast agent [181]. This manganese oxide nanoparticle formulation was successfully used to image transplanted cells, but was characterized by a lower sensitivity that was inferior to that of iron oxide [182]. A modification toward mesoporous silica-coated hollow manganese oxide nanoparticles yielded increased T1 signal through better access of water molecules to the magnetic core [183].

7.1.1.1.4. Fluorine nanoparticles: Fluorine is a chemical element that is practically absent in the human body; thus, ^{19}F imaging can be used to produce contrast devoid of any tissue background. Another advantage of this method is that, during the same imaging session, both ^{1}H anatomical and ^{19}F "hot spot" images can be acquired and superimposed [184], providing data in a quantitative manner[185]. While the signal-to-noise ratio (SNR) of ^{19}F is about 89% that of ^{1}H per nucleus, the fluorine-based contrast agent requires a very high density of ^{19}F nuclei, similar to that of ^{1}H density in tissues[186]. This has been accomplished by synthesizing fluorine compounds from hydrocarbons through the exchange of ^{1}H to ^{19}F nuclei[187]. Even prior to the era of MRI, fluorocarbons were used as an X-ray contrast agent [188], or as a blood substitute [189]. Thus, the biocompatibility of fluorocarbons is undoubted. Perfluoropolyether nanoparticles have been successfully used to track dendritic cells [190], pancreatic islets [191], and neural stem cells (Fig. 3) [192,193]. While perfluorocarbon is a very promising contrast agent for "hot spot" MRI, its utility is still limited by the low sensitivity of the method [194], requiring a significant amount of cells for in vivo imaging [195].

7.1.1.1.5. PARACEST nanoparticles: Chemical exchange saturation transfer (CEST) is a new contrast mechanism based on the exchange of protons between certain molecules and bulk water as the result of saturation with an off-resonance pulse sequence, or the use of rare earth metals that provide a paramagnetic shift in the resonance frequency (PARACEST). The advantage of PARACEST contrast is that it is saturation pulse frequency-specific, and thus, completely switch-able, and contrast is generated only after applying a specific saturation pulse. As such, CEST does not interfere with other MR parameters, i.e., T2, T1, or diffusion. The sensitivity of CEST for proteins and polymers is very low; however, the use of PARACEST has been shown to produce a stronger signal. Chelates of europium and ytterbium were shown to be good PARACEST agents, and these chelates, incorporated into dendrimer nanoparticles, have been used in vivo [196]. PARACEST nanoparticles, as yet, have not been used specifically for stem cell tracking, but this technology is ready to be tested for cell transplantation pending sufficient sensitivity of detection.

7.1.1.1.6. Gold and tantalum nanoparticles: Heavy metals have long been used as contrast agents for electron microscopy [197–199]. The biocompatibility of gold has already been established in dentistry[200,201] and the low cytotoxicity of cell labeling with gold nanoparticles has been confirmed in vitro [202]. Just a few years ago, it was reported that gold nanoparticles were characterized by very high X-ray absorption, far beyond iodinated compounds, confirming that these particles made good X-ray contrast agents, when systemically delivered in small [203] and large animals [204]. Only recently, successful tracking of cells labeled with gold nanoparticles using micro-CT has been shown [84]. As discussed above, gold has many features advantageous for cellular imaging; however, a significant disadvantage is its cost. Thus, there was an effort to replace it with low-cost, bio-inert tantalum oxide nanoparticles, which reportedly have the many advantages of gold nanoparticles, including low toxicity [205,206].

7.1.1.1.7. Quantum dots: The term “quantum dots” has been coined for three-dimensionally confined semiconductor nanocrystals [207]. These nanocrystals are characterized by a stable and unique fluorescence emission band that is easily tunable by manipulating the size or the composition of crystals [208]. The broad absorption and narrowemission bands facilitate multicolor imaging of dynamic cellular events[209]. The production of quantum dots with an emission spectrum in the near infrared range contributes to their use for in vivo imaging[210,211], including successful tracking of stem cells transplanted into the brain [212,213]. It has been shown that near infrared quantum dots (QD 800) produce a higher in vivo signal compared to far red quantum dots (QD 655) [214]. Toxicity studies have demonstrated that quantum dots have no effect on the viability, proliferation, or differentiation potential of stem cells [215]; however, pro-thrombotic adverse events were reported following intravenous transplantation of labeled mesenchymal stem cells [216].

7.1.1.1.8. Polymer dots: Highly fluorescent, π-conjugated, polymer-based semiconductor nanoparticles are an organic alternative to quantum dots [217]. These nanoparticles are characterized by a very high emission rate, minimal “blinking” behavior, and excellent photostability. Various polymers emit photons of distinct wave-lengths, which enable multicolor imaging. Recent advances toward the construction of near-infrared π-conjugated polymers herald alternative strategy to quantum dots [218]. The successful synthesis inorganic-organic/nanocrystals-polymer hybrids with unique properties has also been reported, which may further enhance the detection of transplanted cells [219].

7.1.1.1.9. Nanodiamonds: Among the diversity of biolabels, fluorescent nanodiamonds are also worth mentioning. They have not yet been used for in vivo tracking of stem cells, but their characteristics, such as photostability, chemical non-reactivity, biocompatibility, and emission in the far-red bandwidth, make them another interesting nanoparticle for non-invasive imaging [220]. The atomic compositionof nanodiamonds enables enhancement by fluorescence resonance energy transfer (FRET), but at the cost of the introduction of another label into the cells [221,222]. Nanodiamonds were shown to be relatively safe for the cells [223,224]; however, a slight increase in DNA repair proteins in nanodiamond-labeled embryonic stem cells has been reported [225].

7.1.1.1.10. Upconverting luminescence (UCL) nanoparticles: While near infrared fluorescent nanostructures proved to be useful for in vivo imaging, the autofluorescence is a factor that limits the sensitivity of this method. The process of UCL may help with that limitation. The phenomenon of UCL takes place when absorption of light by the molecule results in the emission of photons with a higher energy, but a shorter wavelength, described as the Anti-Stokes emission process. This phenomenon has been known for many years, but only recently have nanoparticles with such properties, suitable for in vivo applications, been produced. Since there are few, if any, endogenous biological materials that display an upconverted emission, the images obtained by the use of such materials are completely devoid of back-ground [226]. Rare-earth nanophosphors, with upconversion within the near infrared range (both absorption/emission), were used as photoluminescent probes for small animal in vivo bioimaging [227]. Tissue phantoms provided proof-of-principle for cellular imaging, using NaYF4 nanocrystals doped with Tm^{3+}, with detection reaching 3 mm in depth [228]. Very recently, the replacement of yttrium with lutetium, resulting in cubic sub-20 nm NaLuF4-based upconversion nanophosphors, demonstrated a dramatic increase in signal, enabling in vivo imaging of large animals, such as rabbits and pigs [229].

7.1.1.1.11. Nanobubbles: For years, echogenic bubbles have been used as an ultrasonic contrast agent [230,231]. The second harmonic wave provided a background-free signal using an ultrasonic device[232]. Since the frequency of the second harmonic wave was

dependent upon the bubble diameter, the size of the bubbles had to be tuned to the frequency of clinical ultrasonic devices. Based on these calculations, the dimension of bubbles suitable for this application would be in the range of micrometers, and products of this size are being manufactured and are commercially available. However, these preparations are actually oversized and not suitable for intracellular labeling.

Although standard ultrasonography equipment cannot be used to detect cells labeled with nanobubbles, it has been shown that nanobubble-labeled liver cells are detectable by ultrasound microscopy [233]. However, the exposure of the cells to nanobubbles was related to toxicity from some of the bubble formulations; thus, their implementation into clinical practice should be undertaken with caution [234]. Nevertheless, the progress in the formation of stable nanobubbles in a well-controlled manner [235,236] may facilitate the introduction of ultrasonography as a viable strategy for cellular imaging.

7.1.1.2. Multimodal nanoparticles

7.1.1.2.1. Homogenous nanoparticles: Several substances are characterized by their production of contrast that is detectable by more than one imaging modality. Such approach with exploiting one nano-structure for multimodal imaging is particularly useful, with only few reported applications.

Europium-doped mesoporous gadolinium oxide nanoparticles, in addition to MRI signal, are also characterized by strong phosphorescence, which is useful for optical imaging, and these nanoparticles have already been applied to the labeling of HeLa cells [237]. Doping of gadolinium oxide with La^{3+} ions provides an additional upconversion luminescence effect [238].

While iron oxide is one of the best MR contrast agents in terms of signal change, there are metals with even higher magnetic moments, potentially further increasing the signal. The high magnetic moment of cobalt nanoparticles was shown to be even more efficient in signal generation than iron oxide, but, due to insufficient stability, these particles were not useful for biomedical applications [239]. However, manufacturing a hollow cobalt and platinum (CoPt) alloy overcame the hurdle of stability without the accompanying signal decrease[240]. Such magnetic CoPT nanoparticles were successfully employed for stem cell labeling [241]. The presence of platinum as a component of this CoPt alloy renders these particles X-ray visible. It has also been shown that CoPt nanoparticles can be prepared using a dendrimer matrix [242].

Radionuclides are frequently used for stem cell imaging. Due to the very high sensitivity of radionuclides, only a minimal amount of label is necessary, and chemical complexes such as In^{111}-inoxine can be used for cell tracking over the time until the decay of radioactivity, which, in the case of In^{111} is several days [243]. Nanotechnology contributed much to the field of stem cell research with the introduction of multimodal nanoparticles, and by the addition of radionuclides to existing nanoparticles. Since the relatively fast decay process precludes the storage of the radionuclides, the synthesis of such nanoparticles should be as straightforward as possible to enable on-site synthesis immediately prior to their application. To meet these requirements, rapid, size-controlled synthesis of dextran-coated ^{64}Cu-doped iron oxide nanoparticles has been developed using simple microwaving [244].

Perfluorooctylbromide, in addition to the MRI signal of fluorine, is also characterized by strong X-ray absorption due to the presence of bromide atoms, making it suitable for CT imaging [191]. Perfluoropropane nanobubbles, in turn, are used for ultrasound imaging and are also visible on ^{19}F MRI [245].

7.1.1.2.2. Hybrid nanoparticles: While there are only a few examples of tracers made from homogenous multimodal nanoparticles, there are numerous hybrid nanoparticles employed for multimodal stem cell tracking (Table 1). Usually, these hybrids are composed of two or more substances used for unimodal nanostructures, or with one nanostructure and an additional optical dye or/and radionuclide. The core of such a unimodal nanoparticle is typically surrounded by a shell made of another unimodal material. An iron oxide core coated with a gold shell exemplifies the types of nanoparticles designed for dual MR and CT imaging [246,247]. A more advanced design includes a CT-visible core made of perfluorooctylbromide with a conjugated europium chelate that produces a CEST MRI signal [248]. Fluorescein[249] or rhodamine [250] bound to gadolinium nanoparticles enable both magnetic resonance and optical imaging. An attractive in vivo stem cell tracking system for clinical translation would be the integration of magnetic nanoparticles with near infrared quantum dots[251]. Attaching Cy5.5 to iron oxide nanoparticles also enables both MR and NIR imaging [252,253]. Dendrimer-based nanoparticles can be coated with various labels, including gadolinium and Cy5.5 [254]. Triple-modality nanoparticles, with a heavy metal core coated with paramagnetic and optical tags, have also been described (Fig. 4) [255].

7.1.2. Nanotechnology to enhance cell tracking by reporter genes—Reporter genes have been found to be very useful for identifying transplanted cells [115]. The application of reporter gene-based imaging methods allows for unambiguous conclusions about the viability of transplanted cells. In contrast to many nanoparticles, reporter proteins produced by engineered cells are very short-lived and degrade rapidly following cell death, with a resulting loss of signal. They are also resistant to contrast dilution during cell proliferation [94]. The most popular reporter genes that are suitable for in vivo imaging in small animals are based on light-emitting proteins or enzymes. The recent discovery of reporter genes with fluorescent protein emitting in the near-infrared range may open up applications for optical imaging in large animals or even in humans [256]. However, the clinical application of reporter genes for stem cell tracking faces some challenges, including the safety issues associated with manipulating the genome or the effects of gene introduction into the cells. While the in vivo gene therapy of malignant tumors [257,258] or the ex vivo introduction of reporter genes to therapeutic immune cells [259] have been used, the genetic alteration of stem cells in regenerative medicine, due to their expected long-term survival, has met with much more resistance. Efficient gene delivery to human therapeutic stem cells is still challenging. While transfection/transduction of immune cells or immortalized human stem cells is quite efficient, the genetic modification of primary human cells with therapeutic potential is very difficult. While reporter gene-expressing therapeutic cells can be derived from transgenic 849 donor animals, such a strategy is not applicable for human cells. Thus, there is an effort to improve reporter gene delivery to primary stem cells using developments in nanotechnology. Nano-coating is a very interesting strategy to enhance gene delivery to the cells. The surface coating of individual cells with an amino-acid functionalized calcium phosphate nano-film was initially used with the intention of guiding the process of cell differentiation. The so called “exo-scaffolds,” characterized by a positive charge of hydroxyapatite, were found to significantly enhance non-viral transfection methods, probably by increasing plasmid concentration at the cell surface [260]. Nano-coating with a chitosan and chitosan-hyaluronan was shown to increase the endocytosis of both DNA plasmids and iron oxide nanoparticles [261].

7.2. Extracellular labels and tracers

7.2.1. Encapsulation—The technology of microencapsulation has been developed primarily to protect transplanted cells against an immune attack by the host [262]. Since visualization of transplanted cells is necessary to correctly determine the cell-dependent

effect, it has been proposed that the capsules containing these cells might also be monitored with in vivo imaging. For many years, alginate has been used to encapsulate living cells [263]. The co-encapsulation of pancreatic beta islet cells in alginate capsules with iron oxide [264–266] or barium (sulfate) [267–269] enabled tracking by MRI and CT, respectively. Then, trimodal gadolinium-gold capsules were introduced, with detectability by MRI, CT, and ultrasonography (Fig. 5) [270]. This was achieved by the functionalization of gold nanoparticles with gadolinium chelates and through cross-linking of alginate with clinical-grade protamine sulfate [271]. As some of the nanoparticles with beneficial imaging parameters may be toxic, a strategy has been developed to shield cells from such particles using capsule-in-capsule (CIC) methods, in which nanoparticles are first encapsulated within an internal capsule, and then the cells are incorporated within the external capsule layer, providing a physical separation of cells and nanoparticles [272]. By adding perfluorocarbons to the capsules, a trimodal capsule composition can also be synthesized that can be detected with ^{19}F MRI, CT, and USG [273].

Another approach is to label the capsule wall, as for iron oxide[274] and gadolinium chelates [275]. Particles incorporated into the wall of the capsule demonstrated a sufficient signal for in vivo MRI, and did not expose the cells to the label itself. PEG-lipids used for single-cell encapsulation of HEK293 cells (Fig. 6) [276] and hepatocytes [277] were conjugated with FITC for in vitro visualization. A chitosan-alexa fluor 647 conjugate has been employed for the in vitro imaging of multilayer chitosan/alginate nano-coating of beta islets [278]. A modification of this strategy with the use of near infrared dye could potentially be applicable to clinical capsule imaging.

7.2.2. Nanogels—Nanogels are composed of cross-linked polymer nanoparticles and have been increasingly used as injectable scaffolds for transplanted cells, especially useful in case of cell deposition within cavities. The use of scaffold materials facilitates uniform cell distribution and provides a substrate for cell adhesion [279,280], as well as promoting cell differentiation and survival [281]. It has been shown that the deposition of cells within a hydrogel enhanced the therapeutic effects of the cells in a model of acute kidney injury [282] and myocardial infarction[283,284]. Imaging of nanogels has also been explored, with reports on labeling with fluorescence tags, such as rhodamine B [285] or quantum dots [286,287] or magnetic iron oxide [288]. This strategy with tagging gels that encapsulate therapeutic cells could potentially provide information about whether deposited cells remain within the targeted site or redistribute. Nanogels were also shown to improve the efficiency of cell labeling with quantum dots [289,290] or gold nanoparticles [291].

8. Advances in imaging of labeled cells in vitro

The growing interest in the application of nanotechnologies to cell tracking requires tools by which to evaluate the interactions of nanotracers with living cells at the subcellular level [292]. Coherent anti-Stokes Raman scattering (CARS) microscopy enables the visualization of metal oxide particles based only on their electron density, obviating the need for combination with other labels for in vitro visualization [293,294]. Further advances with the application of stimulated Raman scattering provides such visualization at high temporal resolution, enabling recording at video-rate [295]. Surface-enhanced Raman spectroscopy enabled the imaging of the cellular transport pathways of gold nanoparticles (Fig. 7) [296]. This allows confirmation, in living cells, that the nanoparticles were efficiently internalized, and in which cell compartment these nanoparticles are located.

9. Clinical applications of stem cell tracking

The interest in stem cell therapy is keen, and, over the last decade, has increased dramatically; a search of the clinicaltrials.gov database on 03/24/2012, using the key word "stem cells," returned a stunning 3,971 records. As presented in this review, there is a multitude of techniques for tracking cells, some suitable only for the laboratory setting, but some with clinical translation potential. To date, only 19 clinical trials (which included a total of 145 patients) have reported the use of stem cell tracking [297]. Nuclear medicine was a dominating modality with the majority of applications in the field of cardiology. Contrast materials used for these studies were either 111-indium and 99-technetium chelates or 18-FDG. Thus, all nuclear medicine applications did not use nanotechnology approaches.

Iron oxide nanoparticles have been the only nanostructures used in a clinical setting [298–301]. Considering the abundance of nanomaterials, the low rate of clinical translation is somewhat surprising and disappointing, particularly if patients could greatly benefit from more targeted and personalized stem cell therapies. Further research on the biocompatibility and safety of the most promising agents should help in the rapid translation of new nanotechnology developments.

10. Limitations

While the enthusiasm related to the biomedical applications of nanotechnology is substantial, these approaches are not devoid of risk, which requires careful planning and preclinical testing before wide clinical application. Some nanomaterials that were envisioned to be highly useful therapeutically proved toxic, including such agents as carbon nanotubes [302], as well as silver [303] and copper nanoparticles [304,305]. The toxicity may even depend on the size of the material, as was shown for gold nanoparticles with intraperitoneal injection. In this instance, 17 nm particles led to impaired cognition in mice, while such an effect was not observed after the application of larger 37 nm gold nanoparticles [306]. Gold nanoparticles are known to generate heat after exposure to near infrared light [307] or ionizing radiation [308], which is actually used in cancer therapy, but which may interfere with diagnostic imaging. Transplanted stem cells are meant to function over extended periods of time; thus, the evaluation of potential toxic effects should be performed for both immediate and long-term effects. It has been shown that even if no acute side effects are observed, some particles may cause an inflammatory response during long-term observation [309], inhibit chondrogenesis [310,311], or temporarily interfere with the speed of migration [312].

It is not only the safety, but also the reliability of stem cell tracking methods that should be considered. The interpretation of in vivo imaging can be complicated by such processes as contrast dilution following cell division [115,313], uptake of the label by phagocytes following the death of transplanted cells, or, as has been recently reported, transfer of magnetic nanoparticles via microvesicles due to stress (starvation) [314].

11. Summary

Current treatment methods for many diseases are ineffective and inadequate, thus driving the growing interest in stem cell therapy. The implementation of personalized medicine, based on extensive and accurate individual patient data, opens up the possibility to design therapy more specifically, customizing it to the needs of each particular patient. This approach heralds a more tailored and likely more efficient use of stem cells. The ability to non-invasively, monitor the fate of transplanted cells, in real-time, is a crucial requirement to conduct experimental therapies, and only that ability can provide meaningful data that will allow the advancement of cell therapy. The advent of nanotechnology boosts the arsenal of

methods for tracking stem cells in patients. Thus, investigators and clinicians who introduce cell therapies into the clinical realm should be knowledgeable and able to briskly navigate between the available methods of cell tracking so as to customize the protocol for each individual case. In general, the selection of the imaging modality and stem cell tracer or label should be based on the primary disorder, but co-morbidities must also be considered, which may influence which modality is best for the individual patient so as to avoid interference with the imaging techniques necessary to evaluate disease progression or recovery. The condition of the patient is also an important factor, as a worse prognosis may justify a treatment strategy that is riskier but has the potential to provide greater benefit, such as cell therapy with the use of cell tracking. At this early stage of the field of cell therapy, randomized trials, because of the inherent within-population heterogeneity, do not seem to be the best strategy. Rather, a personalized approach to treatment appears more appropriate.

The power of personalized nanomedicine lies in the diversity of nanomaterials, which enable individualized tailoring of materials to the specific needs of each patient. The successful implementation of stem cell tracking will likely be a significant driving force that will contribute to the further development of nanotheranostics [315].

Acknowledgments

The authors are supported by 2RO1 NS045062 JWMB, RO1 DA026299, U54 CA151838, MSCRFII-0193, MSCRFII0052, and a Kolumb Fellowship from the Foundation for Polish Science (MJ). The authors thank Mary McAllister for editorial assistance.

References

[1]. Tarrant C, Windridge K, Boulton M, Baker R, Freeman G. How important is personal care in general practice? BMJ. 2003; 326:1310. [PubMed: 12805168]

[2]. Kearley KE, Freeman GK, Heath A. An exploration of the value of the personal doctor–patient relationship in general practice. Br. J. Gen. Pract. 2001; 51:712–718. [PubMed: 11593831]

[3]. Ridd M, Shaw A, Lewis G, Salisbury C. The patient–doctor relationship: a synthesis of the qualitative literature on patients' perspectives. Br. J. Gen. Pract. 2009; 59:e116–e133. [PubMed: 19341547]

[4]. Hood L. Biotechnology and medicine of the future. JAMA. 1988; 259:1837–1844. [PubMed: 3278155]

[5]. Meyer UA. Pharmacogenetics—five decades of therapeutic lessons from genetic diversity. Nat. Rev. Genet. 2004; 5:669–676. [PubMed: 15372089]

[6]. Caldwell J. Drug metabolism and pharmacogenetics: the British contribution to fields of international significance. Br. J. Pharmacol. 2006; 147(Suppl. 1):S89–S99. [PubMed: 16402125]

[7]. Kalow W. Perspectives in pharmacogenetics. Arch. Pathol. Lab. Med. 2001; 125:77–80. [PubMed: 11151057]

[8]. Hood L, Hunkapiller M, Hewick R, Giffin CE, Dreyer WJ. Microchemical instrumentation. J. Supramol. Struct. Cell. Biochem. 1981; 17:27–36. [PubMed: 7321052]

[9]. Hood L. A personal journey of discovery: developing technology and changing biology. Annu. Rev. Anal. Chem. (Palo Alto Calif). 2008; 1:1–43. [PubMed: 20636073]

[10]. Tugwell P, Knottnerus JA, Idzerda L. Clinical epidemiologists and EBM proponents need to be able to critically appraise 'Omics', the fatal flaw of Personalized Medicine. J. Clin. Epidemiol. 2010; 63:943–944. [PubMed: 20656192]

[11]. Senn S, Rolfe K, Julious SA. Investigating variability in patient response to treatment—a case study from a replicate cross-over study. Stat. Methods Med. Res. 2011; 20:657–666. [PubMed: 20739334]

[12]. Banta HD. RCTs and the federal government. Control. Clin. Trials. 1982; 3:173–183. [PubMed: 6759032]

[13]. Susce MT, Villanueva N, Diaz FJ, de Leon J. Obesity and associated complications in patients with severe mental illnesses: a cross-sectional survey. J. Clin. Psychiatry. 2005; 66:167–173. [PubMed: 15705001]

[14]. de Leon J. Evidence-based medicine versus personalized medicine: are they enemies? J. Clin. Psychopharmacol. 2012

[15]. Haynes B. ACP Journal Club, Editorial: new and underutilized features of ACP Journal Club PLUS and ACPJC.org: stellar articles, searches, and succinct synopses of the principles and practice of “personalized” evidence-based medicine. Ann. Intern. Med. 2009; 151 (JC6-2, JC6-3).

[16]. Leon AC. Two clinical trial designs to examine personalized treatments for psychiatric disorders. J. Clin. Psychiatry. 2011; 72:593–597. [PubMed: 20673550]

[17]. Danesi R, Mosca M, Boggi U, Mosca F, Del Tacca M. Genetics of drug response to immunosuppressive treatment and prospects for personalized therapy. Mol. Med. Today. 2000; 6:475–482. [PubMed: 11099953]

[18]. Eng G, Chen A, Vess T, Ginsburg G. Genome technologies and personalized dental medicine. Oral Dis. 2012; 18:223–235. [PubMed: 22129463]

[19]. Ginsburg GS, Staples J, Abernethy AP. Academic medical centers: ripe for rapid-learning personalized health care. Sci. Transl. Med. 2011; 3 (101cm127).

[20]. Arnold GL, Vockley J. Thoroughly modern medicine. Mol. Genet. Metab. 2011; 104:1–2. [PubMed: 21807540]

[21]. Janowski M, Lukomska B, Domanska-Janik K. Migratory capabilities of human umbilical cord blood-derived neural stem cells (HUCB-NSC) in vitro. Acta Neurobiol. Exp. (Wars). 2011; 71:24–35. [PubMed: 21499324]

[22]. Lindvall O. Transplantation into the human brain: present status and future possibilities. J. Neurol. Neurosurg. Psychiatry. 1989; (Suppl.):39–54. [PubMed: 2666578]

[23]. Lindvall O, Rehncrona S, Brundin P, Gustavii B, Astedt B, Widner H, Lindholm T, Bjorklund A, Leenders KL, Rothwell JC, Frackowiak R, Marsden D, Johnels B, Steg G, Freedman R, Hoffer BJ, Seiger A, Bygdeman M, Stromberg I, Olson L. Human fetal dopamine neurons grafted into the striatum in two patients with severe Parkinson’s disease. A detailed account of methodology and a 6-month follow-up. Arch. Neurol. 1989; 46:615–631. [PubMed: 2786405]

[24]. Piscaglia AC. Stem cells, a two-edged sword: risks and potentials of regenerative medicine. World J. Gastroenterol. 2008; 14:4273–4279. [PubMed: 18666313]

[25]. Robinton DA, Daley GQ. The promise of induced pluripotent stem cells in research and therapy. Nature. 2012; 481:295–305. [PubMed: 22258608]

[26]. Bednar MM, Perry A. Neurorestoration therapeutics for neurodegenerative and psychiatric disease. Neurol. Res. 2012

[27]. Ebben JD, Zorniak M, Clark PA, Kuo JS. Introduction to induced pluripotent stem cells: advancing the potential for personalized medicine. World Neurosurg. 2011; 76:270–275. [PubMed: 21986423]

[28]. Lindvall O, Brundin P, Widner H, Rehncrona S, Gustavii B, Frackowiak R, Leenders KL, Sawle G, Rothwell JC, Marsden CD, et al. Grafts of fetal dopamine neurons survive and improve motor function in Parkinson’s disease. Science. 1990; 247:574–577. [PubMed: 2105529]

[29]. Lindvall O, Widner H, Rehncrona S, Brundin P, Odin P, Gustavii B, Frackowiak R, Leenders KL, Sawle G, Rothwell JC, et al. Transplantation of fetal dopamine neurons in Parkinson’s disease: one-year clinical and neurophysiological observations in two patients with putaminal implants. Ann. Neurol. 1992; 31:155–165. [PubMed: 1575454]

[30]. Olanow CW, Goetz CG, Kordower JH, Stoessl AJ, Sossi V, Brin MF, Shannon KM, Nauert GM, Perl DP, Godbold J, Freeman TB. A double-blind controlled trial of bilateral fetal nigral transplantation in Parkinson’s disease. Ann. Neurol. 2003; 54:403–414. [PubMed: 12953276]

[31]. Freed CR, Greene PE, Breeze RE, Tsai WY, DuMouchel W, Kao R, Dillon S, Winfield H, Culver S, Trojanowski JQ, Eidelberg D, Fahn S. Transplantation of embryonic dopamine neurons for severe Parkinson’s disease. N. Engl. J. Med. 2001; 344:710–719. [PubMed: 11236774]

[32]. Bertz H, Spyridonidis A, Ihorst G, Engelhardt M, Grullich C, Wasch R, Marks R, Finke J. Marrow versus blood-derived stem cell grafts for allogeneic transplantation from unrelated

donors in patients with active myeloid leukemia or myelodysplasia. Biol. Blood Marrow Transplant. 2011

[33]. Sanz J, Boluda JC, Martin C, Gonzalez M, Ferra C, Serrano D, de Heredia CD, Barrenetxea C, Martinez AM, Solano C, Sanz MA, Sanz GF. Single-unit umbilical cord blood transplantation from unrelated donors in patients with hematological malignancy using busulfan, thiotepa, fludarabine and ATG as myeloablative conditioning regimen. Bone Marrow Transplant. 2012

[34]. Bacigalupo A. Treatment strategies for patients with severe aplastic anemia. Bone Marrow Transplant. 2008; 42(Suppl. 1):S42–S44. [PubMed: 18724299]

[35]. Marsh JC. Management of acquired aplastic anaemia. Blood Rev. 2005; 19:143–151. [PubMed: 15748962]

[36]. Addis RC, Bulte JW, Gearhart JD. Special cells, special considerations: the challenges of bringing embryonic stem cells from the laboratory to the clinic. Clin. Pharmacol. Ther. 2008; 83:386–389. [PubMed: 18285783]

[37]. Muja N, Bulte JW. Magnetic resonance imaging of cells in experimental disease models. Prog. Nucl. Magn. Reson. Spectrosc. 2009; 55:61–77. [PubMed: 21552511]

[38]. Long CM, Bulte JW. In vivo tracking of cellular therapeutics using magnetic resonance imaging. Expert Opin. Biol. Ther. 2009; 9:293–306. [PubMed: 19216619]

[39]. Russ HA, Efrat S. Development of human insulin-producing cells for cell therapy of diabetes. Pediatr. Endocrinol. Rev. 2011; 9:590–597. [PubMed: 22397143]

[40]. Hughes RD, Mitry RR, Dhawan A. Current status of hepatocyte transplantation. Transplantation. 2012; 93:342–347. [PubMed: 22082820]

[41]. Matsumoto S. Islet cell transplantation for Type 1 diabetes. J. Diabetes. 2010; 2:16–22. [PubMed: 20923470]

[42]. Zhang Q, Yang Y, Zhang J, Wang GY, Liu W, Qiu DB, Hei ZQ, Ying QL, Chen GH. Efficient derivation of functional hepatocytes from mouse induced pluripotent stem cells by a combination of cytokines and sodium butyrate. Chin. Med. J. (Engl). 2011; 124:3786–3793. [PubMed: 22340242]

[43]. Bin WT, Ma LM, Xu Q, Shi XL. Embryonic hepatocyte transplantation for hepatic cirrhosis: efficacy and mechanism of action. World J. Gastroenterol. 2012; 18:309–322. [PubMed: 22294837]

[44]. Bukong TN, Lo T, Szabo G, Dolganiuc A. Novel developmental biology-based protocol of embryonic stem cell differentiation to morphologically sound and functional yet immature hepatocytes. Liver Int. 2012

[45]. am Esch JS, Schmelzle M, Furst G, Robson SC, Krieg A, Duhme C, Tustas RY, Alexander A, Klein HM, Topp SA, Bode JG, Haussinger D, Eisenberger CF, Knoefel WT. Infusion of CD133+ bone marrow-derived stem cells after selective portal vein embolization enhances functional hepatic reserves after extended right hepatectomy: a retrospective single-center study. Ann. Surg. 2012; 255:79–85. [PubMed: 22156926]

[46]. Lee HJ, Selesniemi K, Niikura Y, Niikura T, Klein R, Dombkowski DM, Tilly JL. Bone marrow transplantation generates immature oocytes and rescues long-term fertility in a preclinical mouse model of chemotherapy-induced premature ovarian failure. J. Clin. Oncol. 2007; 25:3198–3204. [PubMed: 17664466]

[47]. Ch'ang HJ, Lin LM, Chang PY, Luo CW, Chang YH, Chou CK, Chen HH. Bone marrow transplantation enhances trafficking of host-derived myelomonocytic cells that rescue intestinal mucosa after whole body radiation. Radiother. Oncol. 2012

[48]. Brenner H, Ahern W. Sickness absence and early retirement on health grounds in the construction industry in Ireland. Occup. Environ. Med. 2000; 57:615–620. [PubMed: 10935942]

[49]. Murtezani A, Hundozi H, Orovcanec N, Berisha M, Meka V. Low back pain predict sickness absence among power plant workers. Indian J. Occup. Environ. Med. 2010; 14:49–53. [PubMed: 21120081]

[50]. Pacini S, Spinabella S, Trombi L, Fazzi R, Galimberti S, Dini F, Carlucci F, Petrini M. Suspension of bone marrow-derived undifferentiated mesenchymal stromal cells for repair of superficial digital flexor tendon in race horses. Tissue Eng. 2007; 13:2949–2955. [PubMed: 17919069]

[51]. Godwin EE, Young NJ, Dudhia J, Beamish IC, Smith RK. Implantation of bone marrow-derived mesenchymal stem cells demonstrates improved outcome in horses with overstrain injury of the superficial digital flexor tendon. Equine Vet. J. 2012; 44:25–32. [PubMed: 21615465]

[52]. Jungebluth P, Alici E, Baiguera S, Blanc K. Le, Blomberg P, Bozoky B, Crowley C, Einarsson O, Grinnemo KH, Gudbjartsson T, Le Guyader S, Henriksson G, Hermanson O, Juto JE, Leidner B, Lilja T, Liska J, Luedde T, Lundin V, Moll G, Nilsson B, Roderburg C, Stromblad S, Sutlu T, Teixeira AI, Watz E, Seifalian A, Macchiarini P. Tracheobronchial transplantation with a stem-cell-seeded bioartificial nanocomposite: a proof-of-concept study. Lancet. 2011; 378:1997–2004. [PubMed: 22119609]

[53]. Biswas A, Bayer IS, Biris AS, Wang T, Dervishi E, Faupel F. Advances in top-down and bottom-up surface nanofabrication: techniques, applications & future prospects. Adv. Colloid Interface Sci. 2012; 170:2–27. [PubMed: 22154364]

[54]. Sugimoto Y, Pou P, Custance O, Jelinek P, Abe M, Perez R, Morita S. Complex patterning by vertical interchange atom manipulation using atomic force microscopy. Science. 2008; 322:413–417. [PubMed: 18927388]

[55]. Mascaro, A.L. Allegra; Sacconi, L.; Pavone, FS. Multi-photon nanosurgery in live brain. Front Neuroenerg. 2010; 2

[56]. Lin Y, Mao C. Bio-inspired supramolecular self-assembly towards soft nanomaterials. Front. Mater. Sci. 2011; 5:247–265. [PubMed: 21980594]

[57]. Itojima Y, Ogawa Y, Tsuno K, Handa N, Yanagawa H. Spontaneous formation of helical structures from phospholipid–nucleoside conjugates. Biochemistry. 1992; 31:4757–4765. [PubMed: 1591237]

[58]. Wang L, Prozorov T, Palo PE, Liu X, Vaknin D, Prozorov R, Mallapragada S, Nilsen-Hamilton M. Self-assembly and biphasic iron-binding characteristics of Mms6, a bacterial protein that promotes the formation of superparamagnetic magnetite nanoparticles of uniform size and shape. Biomacromolecules. 2012; 13:98–105. [PubMed: 22112204]

[59]. Huang HC, Chang PY, Chang K, Chen CY, Lin CW, Chen JH, Mou CY, Chang ZF, Chang FH. Formulation of novel lipid-coated magnetic nanoparticles as the probe for in vivo imaging. J. Biomed. Sci. 2009; 16:86. [PubMed: 19772552]

[60]. Yue-Jian C, Juan T, Fei X, Jia-Bi Z, Ning G, Yi-Hua Z, Ye D, Liang G. Synthesis, self-assembly, and characterization of PEG-coated iron oxide nanoparticles as potential MRI contrast agent. Drug Dev. Ind. Pharm. 2010; 36:1235–1244. [PubMed: 20818962]

[61]. Krol S, del Guerra S, Grupillo M, Diaspro A, Gliozzi A, Marchetti P. Multilayer nanoencapsulation. New approach for immune protection of human pancreatic islets. Nano Lett. 2006; 6:1933–1939. [PubMed: 16968004]

[62]. Veerabadran NG, Goli PL, Stewart-Clark SS, Lvov YM, Mills DK. Nanoencapsulation of stem cells within polyelectrolyte multilayer shells. Macromol. Biosci. 2007; 7:877–882. [PubMed: 17599337]

[63]. McAllister K, Sazani P, Adam M, Cho MJ, Rubinstein M, Samulski RJ, DeSimone JM. Polymeric nanogels produced via inverse microemulsion polymerization as potential gene and antisense delivery agents. J. Am. Chem. Soc. 2002; 124:15198–15207. [PubMed: 12487595]

[64]. Dubsky M, Kubinova S, Sirc J, Voska L, Zajicek R, Zajicova A, Lesny P, Jirkovska A, Michalek J, Munzarova M, Holan V, Sykova E. Nanofibers prepared by needleless electrospinning technology as scaffolds for wound healing. J. Mater. Sci. Mater. Med. 2012

[65]. Yoshimoto H, Shin YM, Terai H, Vacanti JP. A biodegradable nanofiber scaffold by electrospinning and its potential for bone tissue engineering. Biomaterials. 2003; 24:2077–2082. [PubMed: 12628828]

[66]. Shimanovich U, Volkov V, Eliaz D, Aizer A, Michaeli S, Gedanken A. Stabilizing RNA by the sonochemical formation of RNA nanospheres. Small. 2011; 7:1068–1074. [PubMed: 21456085]

[67]. Sumer B, Gao J. Theranostic nanomedicine for cancer. Nanomedicine (Lond.). 2008; 3:137–140. [PubMed: 18373419]

[68]. Vizirianakis IS. Nanomedicine and personalized medicine toward the application of pharmacotyping in clinical practice to improve drug-delivery outcomes. Nanomedicine. 2011; 7:11–17. [PubMed: 21094279]

[69]. Brouard M, Barrandon Y. Controlling skin morphogenesis: hope and despair. Curr. Opin. Biotechnol. 2003; 14:520–525. [PubMed: 14580583]

[70]. Kuemmerle HP. Basic problems of clinical pharmacology and toxicology—general pharmacodynamics and pharmacokinetics. Chemotherapy. 1966; 11:142–147. [PubMed: 5958011]

[71]. Ashwal S, Obenaus A, Snyder EY. Neuroimaging as a basis for rational stem cell therapy. Pediatr. Neurol. 2009; 40:227–236. [PubMed: 19218036]

[72]. Bulte JW. In vivo MRI cell tracking: clinical studies. AJR Am. J. Roentgenol. 2009; 193:314–325. [PubMed: 19620426]

[73]. Janowski M, Walczak P, Date I. Intravenous route of cell delivery for treatment of neurological disorders: a meta-analysis of preclinical results. Stem Cells Dev. 2010; 19:5–16. [PubMed: 19951197]

[74]. Janowski M, Date I. Systemic neurotransplantation—a problem-oriented systematic review. Rev. Neurosci. 2009; 20:39–60. [PubMed: 19526733]

[75]. Srinivas M, Aarntzen EH, Bulte JW, Oyen WJ, Heerschap A, de Vries IJ, Figdor CG. Imaging of cellular therapies. Adv. Drug Deliv. Rev. 2010; 62:1080–1093. [PubMed: 20800081]

[76]. de Vries IJ, Lesterhuis WJ, Barentsz JO, Verdijk P, van Krieken JH, Boerman OC, Oyen WJ, Bonenkamp JJ, Boezeman JB, Adema GJ, Bulte JW, Scheenen TW, Punt CJ, Heerschap A, Figdor CG. Magnetic resonance tracking of dendritic cells in melanoma patients for monitoring of cellular therapy. Nat. Biotechnol. 2005; 23:1407–1413. [PubMed: 16258544]

[77]. Zhu J, Zhou L, XingWu F. Tracking neural stem cells in patients with brain trauma. N. Engl. J. Med. 2006; 355:2376–2378. [PubMed: 17135597]

[78]. Gilad AA, van Laarhoven HW, McMahon MT, Walczak P, Heerschap A, Neeman M, van Zijl PC, Bulte JW. Feasibility of concurrent dual contrast enhancement using CEST contrast agents and superparamagnetic iron oxide particles. Magn. Reson. Med. 2009; 61:970–974. [PubMed: 19189296]

[79]. Liu G, Bulte JW, Gilad AA. CEST MRI reporter genes. Methods Mol. Biol. 2011; 711:271–280. [PubMed: 21279607]

[80]. Govil A, Calkins H, Spragg DD. Fusion of imaging technologies: how, when, and for whom? J. Interv. Card. Electrophysiol. 2011; 32:195–203. [PubMed: 21964620]

[81]. Kumar S, Ponnazhagan S. Mobilization of bone marrow mesenchymal stem cells in vivo augments bone healing in a mouse model of segmental bone defect. Bone. 2012

[82]. Carroll SH, Wigner NA, Kulkarni N, Johnston-Cox H, Gerstenfeld LC, Ravid K. The A2B adenosine receptor promotes mesenchymal stem cell differentiation to osteoblasts and bone formation in vivo. J. Biol. Chem. 2012

[83]. Hainfeld JF, O'Connor MJ, Dilmanian FA, Slatkin DN, Adams DJ, Smilowitz HM. Micro-CT enables microlocalisation and quantification of Her2-targeted gold nanoparticles within tumour regions. Br. J. Radiol. 2011; 84:526–533. [PubMed: 21081567]

[84]. Menk RH, Schultke E, Hall C, Arfelli F, Astolfo A, Rigon L, Round A, Ataelmannan K, MacDonald SR, Juurlink BH. Gold nanoparticle labeling of cells is a sensitive method to investigate cell distribution and migration in animal models of human disease. Nanomedicine. 2011; 7:647–654. [PubMed: 21333753]

[85]. Ricles LM, Nam SY, Sokolov K, Emelianov SY, Suggs LJ. Function of mesenchymal stem cells following loading of gold nanotracers. Int. J. Nanomedicine. 2011; 6:407–416. [PubMed: 21499430]

[86]. Bulte JW. Science to practice: can CT be performed for multicolor molecular imaging? Radiology. 2010; 256:675–676. [PubMed: 20720064]

[87]. Cormode DP, Roessl E, Thran A, Skajaa T, Gordon RE, Schlomka JP, Fuster V, Fisher EA, Mulder WJ, Proksa R, Fayad ZA. Atherosclerotic plaque composition: analysis with multicolor CT and targeted gold nanoparticles. Radiology. 2010; 256:774–782. [PubMed: 20668118]

[88]. Lee WW, Marinelli B, van der Laan AM, Sena BF, Gorbatov R, Leuschner F, Dutta P, Iwamoto Y, Ueno T, Begieneman MP, Niessen HW, Piek JJ, Vinegoni C, Pittet MJ, Swirski FK, Tawakol A, Di Carli M, Weissleder R, Nahrendorf M. PET/MRI of inflammation in myocardial infarction. J. Am. Coll. Cardiol. 2012; 59:153–163. [PubMed: 22222080]

[89]. Maramraju SH, Smith SD, Junnarkar SS, Schulz D, Stoll S, Ravindranath B, Purschke ML, Rescia S, Southekal S, Pratte JF, Vaska P, Woody CL, Schlyer DJ. Small animal simultaneous PET/MRI: initial experiences in a 9.4 T microMRI. Phys. Med. Biol. 2011; 56:2459–2480. [PubMed: 21441651]

[90]. Welling MM, Duijvestein M, Signore A, van der Weerd L. In vivo biodistribution of stem cells using molecular nuclear medicine imaging. J. Cell. Physiol. 2011; 226:1444–1452. [PubMed: 21413018]

[91]. Strasser H, Marksteiner R, Margreiter E, Mitterberger M, Pinggera GM, Frauscher F, Fussenegger M, Kofler K, Bartsch G. Transurethral ultrasonography-guided injection of adult autologous stem cells versus transurethral endoscopic injection of collagen in treatment of urinary incontinence. World J. Urol. 2007; 25:385–392. [PubMed: 17701044]

[92]. Kuliszewski MA, Fujii H, Liao C, Smith AH, Xie A, Lindner JR, Leong-Poi H. Molecular imaging of endothelial progenitor cell engraftment using contrast-enhanced ultrasound and targeted microbubbles. Cardiovasc. Res. 2009; 83:653–662. [PubMed: 19564152]

[93]. Barbarese E, Ho SY, D'Arrigo JS, Simon RH. Internalization of microbubbles by tumor cells in vivo and in vitro. J. Neurooncol. 1995; 26:25–34. [PubMed: 8583242]

[94]. Gorelik M, Janowski M, Galpoththawela C, Rifkin R, Levy M, Lukomska B, Kerr D, Bulte J, Walczak P. Non-invasive monitoring of immunosuppressive drug efficacy to prevent rejection of intracerebral glial precursor allografts. Cell Transplant. (in press).

[95]. Liang Y, Walczak P, Bulte JW. Comparison of red-shifted firefly luciferase Ppy RE9 and conventional Luc2 as bioluminescence imaging reporter genes for in vivo imaging of stem cells. J. Biomed. Opt. 2012; 17:016004. [PubMed: 22352654]

[96]. Berman SC, Galpoththawela C, Gilad AA, Bulte JW, Walczak P. Long-term MR cell tracking of neural stem cells grafted in immunocompetent versus immuno-deficient mice reveals distinct differences in contrast between live and dead cells. Magn. Reson. Med. 2011; 65:564–574. [PubMed: 20928883]

[97]. Jobsis FF. Noninvasive, infrared monitoring of cerebral and myocardial oxygen sufficiency and circulatory parameters. Science. 1977; 198:1264–1267. [PubMed: 929199]

[98]. Eda H. Near-infrared spectroscopy in studies of brain oxygenation. Curr. Pharm. Biotechnol. 2012

[99]. Duan L, Zhang YJ, Zhu CZ. Quantitative comparison of resting-state functional connectivity derived from fNIRS and fMRI: a simultaneous recording study. Neuroimage. 2012

[100]. Robertson CS, Zager EL, Narayan RK, Handly N, Sharma A, Hanley DF, Garza H, Maloney-Wilensky E, Plaum JM, Koenig CH, Johnson A, Morgan T. Clinical evaluation of a portable near-infrared device for detection of traumatic intracranial hematomas. J. Neurotrauma. 2010; 27:1597–1604. [PubMed: 20568959]

[101]. Chen G, Ohulchanskyy TY, Liu S, Law WC, Wu F, Swihart MT, Agren H, Prasad PN. Core/Shell NaGdF4:Nd3+/NaGdF4 nanocrystals with efficient near-infrared to near-infrared downconversion photoluminescence for bioimaging applications. ACS Nano. 2012

[102]. Berman, S.M. Cromer; Walczak, P.; Bulte, JW. Tracking stem cells using magnetic nanoparticles. Wiley Interdiscip. Rev. Nanomed. Nanobiotechnol. 2011; 3:343–355. [PubMed: 21472999]

[103]. Bulte JW, Ben-Hur T, Miller BR, Mizrachi-Kol R, Einstein O, Reinhartz E, Zywicke HA, Douglas T, Frank JA. MR microscopy of magnetically labeled neurospheres transplanted into the Lewis EAE rat brain. Magn. Reson. Med. 2003; 50:201–205. [PubMed: 12815696]

[104]. Ben-Hur T, van Heeswijk RB, Einstein O, Aharonowiz M, Xue R, Frost EE, Mori S, Reubinoff BE, Bulte JW. Serial in vivo MR tracking of magnetically labeled neural spheres transplanted in chronic EAE mice. Magn. Reson. Med. 2007; 57:164–171. [PubMed: 17191231]

[105]. Muja N, Cohen ME, Zhang J, Kim H, Gilad AA, Walczak P, Ben-Hur T, Bulte JW. Neural precursors exhibit distinctly different patterns of cell migration upon transplantation during either the acute or chronic phase of EAE: a serial MR imaging study. Magn. Reson. Med. 2011; 65:1738–1749. [PubMed: 21305597]

[106]. Watson DJ, Walton RM, Magnitsky SG, Bulte JW, Poptani H, Wolfe JH. Structure-specific patterns of neural stem cell engraftment after transplantation in the adult mouse brain. Hum. Gene Ther. 2006; 17:693–704. [PubMed: 16839269]

[107]. Magnitsky S, Watson DJ, Walton RM, Pickup S, Bulte JW, Wolfe JH, Poptani H. In vivo and ex vivo MRI detection of localized and disseminated neural stem cell grafts in the mouse brain. Neuroimage. 2005; 26:744–754. [PubMed: 15955483]

[108]. Park BN, Shim W, Lee G, Bang OY, An YS, Yoon JK, Ahn YH. Early distribution of intravenously injected mesenchymal stem cells in rats with acute brain trauma evaluated by (99m)Tc-HMPAO labeling. Nucl. Med. Biol. 2011; 38:1175–1182. [PubMed: 21831649]

[109]. Hauger O, Frost EE, van Heeswijk R, Deminiere C, Xue R, Delmas Y, Combe C, Moonen CT, Grenier N, Bulte JW. MR evaluation of the glomerular homing of magnetically labeled mesenchymal stem cells in a rat model of nephropathy. Radiology. 2006; 238:200–210. [PubMed: 16373768]

[110]. Qiu B, Gao F, Walczak P, Zhang J, Kar S, Bulte JW, Yang X. In vivo MR imaging of bone marrow cells trafficking to atherosclerotic plaques. J. Magn. Reson. Imaging. 2007; 26:339–343. [PubMed: 17623878]

[111]. Gao F, Kar S, Zhang J, Qiu B, Walczak P, Larabi M, Xue R, Frost E, Qian Z, Bulte JW, Yang X. MRI of intravenously injected bone marrow cells homing to the site of injured arteries. NMR Biomed. 2007; 20:673–681. [PubMed: 17285682]

[112]. Bos C, Delmas Y, Desmouliere A, Solanilla A, Hauger O, Grosset C, Dubus I, Ivanovic Z, Rosenbaum J, Charbord P, Combe C, Bulte JW, Moonen CT, Ripoche J, Grenier N. In vivo MR imaging of intravascularly injected magnetically labeled mesenchymal stem cells in rat kidney and liver. Radiology. 2004; 233:781–789. [PubMed: 15486216]

[113]. Gorelik M, Orukari I, Wang J, Galpoththawela C, Kim H, Levy M, Gilad AA, Bar-Shir A, Kerr DA, Levchenko A, Bulte JW, Walczak P. Using MRI cell tracking to evaluate targeting of glial precursor cells to inflammatory tissue using the VLA-4 docking receptor. Radiology. (in press).

[114]. Politi LS. MR-based imaging of neural stem cells. Neuroradiology. 2007; 49:523–534. [PubMed: 17345076]

[115]. Walczak P, Kedziorek DA, Gilad AA, Barnett BP, Bulte JW. Applicability and limitations of MR tracking of neural stem cells with asymmetric cell division and rapid turnover: the case of the shiverer dysmyelinated mouse brain. Magn. Reson. Med. 2007; 58:261–269. [PubMed: 17654572]

[116]. Ruggiero A, Thorek DL, Guenoun J, Krestin GP, Bernsen MR. Cell tracking in cardiac repair: what to image and how to image. Eur. Radiol. 2012; 22:189–204. [PubMed: 21735069]

[117]. de Almeida PE, van Rappard JR, Wu JC. In vivo bioluminescence for tracking cell fate and function. Am. J. Physiol. Heart Circ. Physiol. 2011; 301:H663–H671. [PubMed: 21666118]

[118]. Gilad AA, McMahon MT, Walczak P, Winnard PT Jr. Raman V, van Laarhoven HW, Skoglund CM, Bulte JW, van Zijl PC. Artificial reporter gene providing MRI contrast based on proton exchange. Nat. Biotechnol. 2007; 25:217–219. [PubMed: 17259977]

[119]. Iordanova B, Ahrens ET. In vivo magnetic resonance imaging of ferritin-based reporter visualizes native neuroblast migration. Neuroimage. 2012; 59:1004–1012. [PubMed: 21939774]

[120]. Gilad AA, Winnard PT Jr. van Zijl PC, Bulte JW. Developing MR reporter genes: promises and pitfalls. NMR Biomed. 2007; 20:275–290. [PubMed: 17451181]

[121]. Tian GF, Takano T, Lin JH, Wang X, Bekar L, Nedergaard M. Imaging of cortical astrocytes using 2-photon laser scanning microscopy in the intact mouse brain. Adv. Drug Deliv. Rev. 2006; 58:773–787. [PubMed: 17045697]

[122]. Piccini P, Brooks DJ, Bjorklund A, Gunn RN, Grasby PM, Rimoldi O, Brundin P, Hagell P, Rehncrona S, Widner H, Lindvall O. Dopamine release from nigral transplants visualized in vivo in a Parkinson's patient. Nat. Neurosci. 1999; 2:1137–1140. [PubMed: 10570493]

[123]. Piccini P, Pavese N, Hagell P, Reimer J, Bjorklund A, Oertel WH, Quinn NP, Brooks DJ, Lindvall O. Factors affecting the clinical outcome after neural transplantation in Parkinson's disease. Brain. 2005; 128:2977–2986. [PubMed: 16246865]

[124]. Rous P, Beard JW. Selection with the magnet and cultivation of reticulo-endothelial cells (Kupffer cells). J. Exp. Med. 1934; 59:577–591. [PubMed: 19870267]

[125]. Smith FW, Crosher GA. Mascara—an unsuspected cause of magnetic resonance imaging artifact. Magn. Reson. Imaging. 1985; 3:287–289. [PubMed: 4079676]

[126]. Lund G, Wirtschafter JD, Nelson JD, Williams PA. Tattooing of eyelids: magnetic resonance imaging artifacts. J. Ophthalmic Nurs. Technol. 1986; 5:228–230. [PubMed: 3641929]

[127]. Sacco DC, Steiger DA, Bellon EM, Coleman PE, Haacke EM. Artifacts caused by cosmetics in MR imaging of the head. AJR Am. J. Roentgenol. 1987; 148:1001–1004. [PubMed: 3495103]

[128]. Chen W, Cormode DP, Fayad ZA, Mulder WJ. Nanoparticles as magnetic resonance imaging contrast agents for vascular and cardiac diseases, Wiley Interdiscip. Rev. Nanomed. Nanobiotechnol. 2010

[129]. Stark DD, Weissleder R, Elizondo G, Hahn PF, Saini S, Todd LE, Wittenberg J, Ferrucci JT. Superparamagnetic iron oxide: clinical application as a contrast agent for MR imaging of the liver. Radiology. 1988; 168:297–301. [PubMed: 3393649]

[130]. Shapiro EM, Skrtic S, Koretsky AP. Sizing it up: cellular MRI using micron-sized iron oxide particles. Magn. Reson. Med. 2005; 53:329–338. [PubMed: 15678543]

[131]. Pouliquen D, Perdrisot R, Ermias A, Akoka S, Jallet P, Le Jeune JJ. Superparamagnetic iron oxide nanoparticles as a liver MRI contrast agent: contribution of microencapsulation to improved biodistribution. Magn. Reson. Imaging. 1989; 7:619–627. [PubMed: 2630844]

[132]. Bulte JW, Ma LD, Magin RL, Kamman RL, Hulstaert CE, Go KG, The TH, de Leij L. Selective MR imaging of labeled human peripheral blood mononuclear cells by liposome mediated incorporation of dextran-magnetite particles. Magn. Reson. Med. 1993; 29:32–37. [PubMed: 7678318]

[133]. Hawrylak N, Ghosh P, Broadus J, Schlueter C, Greenough WT, Lauterbur PC. Nuclear magnetic resonance (NMR) imaging of iron oxide-labeled neural transplants. Exp. Neurol. 1993; 121:181–192. [PubMed: 8339769]

[134]. Bulte JW, Zhang S, van Gelderen P, Herynek V, Jordan EK, Duncan ID, Frank JA. Neurotransplantation of magnetically labeled oligodendrocyte progenitors: magnetic resonance tracking of cell migration and myelination. Proc. Natl. Acad. Sci. U. S. A. 1999; 96:15256–15261. [PubMed: 10611372]

[135]. Bulte JW, Duncan ID, Frank JA. In vivo magnetic resonance tracking of magnetically labeled cells after transplantation. J. Cereb. Blood Flow Metab. 2002; 22:899–907. [PubMed: 12172375]

[136]. Bulte JW, Zhang SC, van Gelderen P, Herynek V, Jordan EK, Janssen CH, Duncan ID, Frank JA. Magnetically labeled glial cells as cellular MR contrast agents. Acad. Radiol. 2002; 9(Suppl. 1):S148–S150. [PubMed: 12019854]

[137]. Tsuchiya K, Nitta N, Sonoda A, Nitta-Seko A, Ohta S, Otani H, Takahashi M, Murata K, Murase K, Nohara S, Mukaisho K. Histological study of the biodynamics of iron oxide nanoparticles with different diameters. Int. J. Nanomedicine. 2011; 6:1587–1594. [PubMed: 21845049]

[138]. Bulte JW, Kraitchman DL. Iron oxide MR contrast agents for molecular and cellular imaging. NMR Biomed. 2004; 17:484–499. [PubMed: 15526347]

[139]. Karmarkar PV, Kraitchman DL, Izbudak I, Hofmann LV, Amado LC, Fritzges D, Young R, Pittenger M, Bulte JW, Atalar E. MR-trackable intramyocardial injection catheter. Magn. Reson. Med. 2004; 51:1163–1172. [PubMed: 15170836]

[140]. Frank JA, Miller BR, Arbab AS, Zywicke HA, Jordan EK, Lewis BK, Bryant LH Jr. Bulte JW. Clinically applicable labeling of mammalian and stem cells by combining superparamagnetic iron oxides and transfection agents. Radiology. 2003; 228:480–487. [PubMed: 12819345]

[141]. Chen S, Alcantara D, Josephson L. A magnetofluorescent nanoparticle for ex-vivo cell labeling by covalently linking the drugs protamine and feraheme. J. Nanosci. Nanotechnol. 2011; 11:3058–3064. [PubMed: 21776671]

[142]. Castaneda RT, Khurana A, Khan R, Daldrup-Link HE. Labeling stem cells with ferumoxytol, an FDA-approved iron oxide nanoparticle. J. Vis. Exp. 2011:e3482. [PubMed: 22083287]

[143]. Thu MS, Bryant LH, Coppola T, Jordan EK, Budde MD, Lewis BK, Chaudhry A, Ren J, Varma NR, Arbab AS, Frank JA. Self-assembling nanocomplexes by combining ferumoxytol, heparin and protamine for cell tracking by magnetic resonance imaging. Nat. Med. 2012; 18:463–467. [PubMed: 22366951]

[144]. Winter EM, Hogers B, van der Graaf LM, Groot A.C. Gittenberger-de, Poelmann RE, van der Weerd L. Cell tracking using iron oxide fails to distinguish dead from living transplanted cells in the infarcted heart. Magn. Reson. Med. 2010; 63:817–821. [PubMed: 20187188]

[145]. Baligand C, Vauchez K, Fiszman M, Vilquin JT, Carlier PG. Discrepancies between the fate of myoblast xenograft in mouse leg muscle and NMR label persistency after loading with Gd-DTPA or SPIOs. Gene Ther. 2009; 16:734–745. [PubMed: 19282845]

[146]. Qiao H, Zhang H, Zheng Y, Ponde DE, Shen D, Gao F, Bakken AB, Schmitz A, Kung HF, Ferrari VA, Zhou R. Embryonic stem cell grafting in normal and infarcted myocardium: serial assessment with MR imaging and PET dual detection. Radiology. 2009; 250:821–829. [PubMed: 19244049]

[147]. Babic M, Horak D, Jendelova P, Glogarova K, Herynek V, Trchova M, Likavanova K, Lesny P, Pollert E, Hajek M, Sykova E. Poly(N, N-dimethylacrylamide)-coated maghemite nanoparticles for stem cell labeling. Bioconjug. Chem. 2009; 20:283–294. [PubMed: 19238690]

[148]. Zhu XM, Wang YX, Leung KC, Lee SF, Zhao F, Wang DW, Lai JM, Wan C, Cheng CH, Ahuja AT. Enhanced cellular uptake of aminosilane-coated superparamagnetic iron oxide nanoparticles in mammalian cell lines. Int. J. Nanomedicine. 2012; 7:953–964. [PubMed: 22393292]

[149]. Chang YK, Liu YP, Ho JH, Hsu SC, Lee OK. Amine-surface-modified superparamagnetic iron oxide nanoparticles interfere with differentiation of human mesenchymal stem cells. J. Orthop. Res. 2012

[150]. Shi Z, Neoh KG, Kang ET, Shuter B, Wang SC, Poh C, Wang W. Carboxymethyl) chitosan-modified superparamagnetic iron oxide nanoparticles for magnetic resonance imaging of stem cells. ACS Appl. Mater. Interfaces. 2009; 1:328–335. [PubMed: 20353220]

[151]. Delcroix GJ, Jacquart M, Lemaire L, Sindji L, Franconi F, Le Jeune JJ, Montero-Menei CN. Mesenchymal and neural stem cells labeled with HEDP-coated SPIO nanoparticles: in vitro characterization and migration potential in rat brain. Brain Res. 2009; 1255:18–31. [PubMed: 19103182]

[152]. Suh JS, Lee JY, Choi YS, Yu F, Yang V, Lee SJ, Chung CP, Park YJ. Efficient labeling of mesenchymal stem cells using cell permeable magnetic nanoparticles. Biochem. Biophys. Res. Commun. 2009; 379:669–675. [PubMed: 19101509]

[153]. Mailander V, Lorenz MR, Holzapfel V, Musyanovych A, Fuchs K, Wiesneth M, Walther P, Landfester K, Schrezenmeier H. Carboxylated superparamagnetic iron oxide particles label cells intracellularly without transfection agents. Mol. Imaging Biol. 2008; 10:138–146. [PubMed: 18297365]

[154]. Horak D, Babic M, Jendelova P, Herynek V, Trchova M, Pientka Z, Pollert E, Hajek M, Sykova E. D-mannose-modified iron oxide nanoparticles for stem cell labeling. Bioconjug. Chem. 2007; 18:635–644. [PubMed: 17370996]

[155]. Cormode DP, Skajaa GO, Delshad A, Parker N, Jarzyna PA, Calcagno C, Galper MW, Skajaa T, Briley-Saebo KC, Bell HM, Gordon RE, Fayad ZA, Woo SL, Mulder WJ. A versatile and tunable coating strategy allows control of nanocrystal delivery to cell types in the liver. Bioconjug. Chem. 2011; 22:353–361. [PubMed: 21361312]

[156]. Taboada E, Rodriguez E, Roig A, Oro J, Roch A, Muller RN. Relaxometric and magnetic characterization of ultrasmall iron oxide nanoparticles with high magnetization. Evaluation as potential T1 magnetic resonance imaging contrast agents for molecular imaging. Langmuir. 2007; 23:4583–4588. [PubMed: 17355158]

[157]. Kim BH, Lee N, Kim H, An K, Park YI, Choi Y, Shin K, Lee Y, Kwon SG, Na HB, Park JG, Ahn TY, Kim YW, Moon WK, Choi SH, Hyeon T. Large-scale synthesis of uniform and extremely small-sized iron oxide nanoparticles for high-resolution T1 magnetic resonance imaging contrast agents. J. Am. Chem. Soc. 2011; 133:12624–12631. [PubMed: 21744804]

[158]. Chaudeurge A, Wilhelm C, Chen-Tournoux A, Farahmand P, Bellamy V, Autret G, Menager C, Hagege A, Larghero J, Gazeau F, Clement O, Menasche P. Can magnetic targeting of magnetically labeled circulating cells optimize intramyocardial cell retention? Cell Transplant. 2011

[159]. Song M, Kim YJ, Kim YH, Roh J, Kim SU, Yoon BW. Using a neodymium magnet to target delivery of ferumoxide-labeled human neural stem cells in a rat model of focal cerebral ischemia. Hum. Gene Ther. 2010; 21:603–610. [PubMed: 20059319]

[160]. Yanai A, Hafeli UO, Metcalfe AL, Soema P, Addo L, Gregory-Evans CY, Po K, Shan X, Moritz OL, Gregory-Evans K. Focused magnetic stem cell targeting to the retina using superparamagnetic iron oxide nanoparticles. Cell Transplant. 2012

[161]. Carniato F, Tei L, Cossi M, Marchese L, Botta M. A chemical strategy for the relaxivity enhancement of Gd(III) chelates anchored on mesoporous silica nanoparticles. Chemistry. 2010; 16:10727–10734. [PubMed: 20669190]

[162]. Modo M, Cash D, Mellodew K, Williams SC, Fraser SE, Meade TJ, Price J, Hodges H. Tracking transplanted stem cell migration using bifunctional, contrast agent-enhanced, magnetic resonance imaging. Neuroimage. 2002; 17:803–811. [PubMed: 12377155]

[163]. McDonald MA, Watkin KL. Investigations into the physicochemical properties of dextran small particulate gadolinium oxide nanoparticles. Acad. Radiol. 2006; 13:421–427. [PubMed: 16554221]

[164]. Rehor I, Vilimova V, Jendelova P, Kubicek V, Jirak D, Herynek V, Kapcalova M, Kotek J, Cerny J, Hermann P, Lukes I. Phosphonate-titanium dioxide assemblies: platform for multimodal diagnostic-therapeutic nanoprobes. J. Med. Chem. 2011; 54:5185–5194. [PubMed: 21662977]

[165]. Hou S, Tong S, Zhou J, Bao G. Block copolymer-based gadolinium nanoparticles as MRI contrast agents with high T(1) relaxivity. Nanomedicine (Lond.). 2012; 7:211–218. [PubMed: 22339134]

[166]. Hedlund A, Ahren M, Gustafsson H, Abrikossova N, Warntjes M, Jonsson JI, Uvdal K, Engstrom M. GdO nanoparticles in hematopoietic cells for MRI contrast enhancement. Int. J. Nanomedicine. 2011; 6:3233–3240. [PubMed: 22228991]

[167]. Loai Y, Sakib N, Janik R, Foltz WD, Cheng H.L. Margaret. Human aortic endothelial cell labeling with positive contrast gadolinium oxide nanoparticles for cellular magnetic resonance imaging at 7 Tesla. Mol. Imaging. 2011

[168]. Guay-Begin AA, Chevallier P, Faucher L, Turgeon S, Fortin MA. Surface modification of gadolinium oxide thin films and nanoparticles using poly(ethylene glycol)-phosphate. Langmuir. 2012; 28:774–782. [PubMed: 21970413]

[169]. Faucher L, Guay-Begin AA, Lagueux J, Cote MF, Petitclerc E, Fortin MA. Ultra-small gadolinium oxide nanoparticles to image brain cancer cells in vivo with MRI. Contrast Media Mol. Imaging. 2011; 6:209–218. [PubMed: 21861281]

[170]. Bhakta G, Sharma RK, Gupta N, Cool S, Nurcombe V, Maitra A. Multifunctional silica nanoparticles with potentials of imaging and gene delivery. Nanomedicine. 2011; 7:472–479. [PubMed: 21215332]

[171]. McDonald MA, Watkin KL. Small particulate gadolinium oxide and gadolinium oxide albumin microspheres as multimodal contrast and therapeutic agents. Invest. Radiol. 2003; 38:305–310. [PubMed: 12908697]

[172]. Tran LA, Krishnamurthy R, Muthupillai R, Mda G. Cabreira-Hansen, Willerson JT, Perin EC, Wilson LJ. Gadonanotubes as magnetic nanolabels for stem cell detection. Biomaterials. 2010; 31:9482–9491. [PubMed: 20965562]

[173]. Anderson SA, Lee KK, Frank JA. Gadolinium-fullerenol as a paramagnetic contrast agent for cellular imaging. Invest. Radiol. 2006; 41:332–338. [PubMed: 16481917]

[174]. Agudelo CA, Tachibana Y, Hurtado AF, Ose T, Iida H, Yamaoka T. The use of magnetic resonance cell tracking to monitor endothelial progenitor cells in a rat hindlimb ischemic model. Biomaterials. 2012; 33:2439–2448. [PubMed: 22206594]

[175]. Koenig SH, Baglin C, Brown RD III, Brewer CF. Magnetic field dependence of solvent proton relaxation induced by Gd3+ and Mn2+ complexes. Magn. Reson. Med. 1984; 1:496–501. [PubMed: 6443784]

[176]. Racette BA, Aschner M, Guilarte TR, Dydak U, Criswell SR, Zheng W. Patho-physiology of manganese-associated neurotoxicity. Neurotoxicology. 2011

[177]. Eriksson H, Tedroff J, Thuomas KA, Aquilonius SM, Hartvig P, Fasth KJ, Bjurling P, Langstrom B, Hedstrom KG, Heilbronn E. Manganese induced brain lesions in Macaca fascicularis as revealed by positron emission tomography and magnetic resonance imaging. Arch. Toxicol. 1992; 66:403–407. [PubMed: 1444804]

[178]. Hussain SM, Javorina AK, Schrand AM, Duhart HM, Ali SF, Schlager JJ. The interaction of manganese nanoparticles with PC-12 cells induces dopamine depletion. Toxicol. Sci. 2006; 92:456–463. [PubMed: 16714391]

[179]. Misselwitz B, Muhler A, Weinmann HJ. A toxicologic risk for using manganese complexes? A literature survey of existing data through several medical specialties. Invest. Radiol. 1995; 30:611–620. [PubMed: 8557501]

[180]. Hussain SM, Hess KL, Gearhart JM, Geiss KT, Schlager JJ. In vitro toxicity of nanoparticles in BRL 3A rat liver cells. Toxicol. In Vitro. 2005; 19:975–983. [PubMed: 16125895]

[181]. Na HB, Lee JH, An K, Park YI, Park M, Lee IS, Nam DH, Kim ST, Kim SH, Kim SW, Lim KH, Kim KS, Kim SO, Hyeon T. Development of a T1 contrast agent for magnetic resonance imaging using MnO nanoparticles. Angew. Chem. Int. Ed Engl. 2007; 46:5397–5401. [PubMed: 17357103]

[182]. Gilad AA, Walczak P, McMahon MT, Na HB, Lee JH, An K, Hyeon T, van Zijl PC, Bulte JW. MR tracking of transplanted cells with “positive contrast” using manganese oxide nanoparticles. Magn. Reson. Med. 2008; 60:1–7. [PubMed: 18581402]

[183]. Kim T, Momin E, Choi J, Yuan K, Zaidi H, Kim J, Park M, Lee N, McMahon MT, Quinones-Hinojosa A, Bulte JW, Hyeon T, Gilad AA. Mesoporous silica-coated hollow manganese oxide nanoparticles as positive T1 contrast agents for labeling and MRI tracking of adipose-derived mesenchymal stem cells. J. Am. Chem. Soc. 2011; 133:2955–2961. [PubMed: 21314118]

[184]. Bulte JW. Hot spot MRI emerges from the background. Nat. Biotechnol. 2005; 23:945–946. [PubMed: 16082363]

[185]. Srinivas M, Heerschap A, Ahrens ET, Figdor CG, de Vries IJ. (19)F MRI for quantitative in vivo cell tracking. Trends Biotechnol. 2010; 28:363–370. [PubMed: 20427096]

[186]. Ruiz-Cabello J, Barnett BP, Bottomley PA, Bulte JW. Fluorine (19F) MRS and MRI in biomedicine. NMR Biomed. 2011; 24:114–129. [PubMed: 20842758]

[187]. Haszeldine RN. Synthesis of fluorocarbons, perfluoroalkyl iodides, bromides and chlorides, and perfluoroalkyl grignard reagents. Nature. 1951; 167:139–140. [PubMed: 14806397]

[188]. Long DM, Liu MS, Szanto PS, Alrenga P. Initial observations with a new X-ray contrast agent–radiopaque perfluorocarbon. Rev. Surg. 1972; 29:71–76. [PubMed: 5011636]

[189]. Tremper KK, Lapin R, Levine E, Friedman A, Shoemaker WC. Hemodynamic and oxygen transport effects of a perfluorochemical blood substitute, fluosol-DA (20%). Crit. Care Med. 1980; 8:738–741. [PubMed: 7449405]

[190]. Ahrens ET, Flores R, Xu H, Morel PA. In vivo imaging platform for tracking immunotherapeutic cells. Nat. Biotechnol. 2005; 23:983–987. [PubMed: 16041364]

[191]. Barnett BP, Ruiz-Cabello J, Hota P, Ouwerkerk R, Shamblott MJ, Lauzon C, Walczak P, Gilson WD, Chacko VP, Kraitchman DL, Arepally A, Bulte JW. Use of perfluorocarbon nanoparticles for non-invasive multimodal cell tracking of human pancreatic islets. Contrast Media Mol. Imaging. 2011; 6:251–259. [PubMed: 21861285]

[192]. Boehm-Sturm P, Mengler L, Wecker S, Hoehn M, Kallur T. In vivo tracking of human neural stem cells with ^{19}F magnetic resonance imaging. PLoS One. 2011; 6:e29040. [PubMed: 22216163]

[193]. Ruiz-Cabello J, Walczak P, Kedziorek DA, Chacko VP, Schmieder AH, Wickline SA, Lanza GM, Bulte JW. In vivo “hot spot” MR imaging of neural stem cells using fluorinated nanoparticles. Magn. Reson. Med. 2008; 60:1506–1511. [PubMed: 19025893]

[194]. Chen J, Lanza GM, Wickline SA. Quantitative magnetic resonance fluorine imaging: today and tomorrow. Wiley Interdiscip. Rev. Nanomed. Nanobiotechnol. 2010; 2:431–440. [PubMed: 20564465]

[195]. Partlow KC, Chen J, Brant JA, Neubauer AM, Meyerrose TE, Creer MH, Nolta JA, Caruthers SD, Lanza GM, Wickline SA. ^{19}F magnetic resonance imaging for stem/progenitor cell tracking with multiple unique perfluorocarbon nanobeacons. FASEB J. 2007; 21:1647–1654. [PubMed: 17284484]

[196]. Ali MM, Yoo B, Pagel MD. Tracking the relative in vivo pharmacokinetics of nanoparticles with PARACEST MRI. Mol. Pharm. 2009; 6:1409–1416. [PubMed: 19298054]

[197]. Juurlink BH, Devon RM. Colloidal gold as a permanent marker of cells. Experientia. 1991; 47:75–77. [PubMed: 1705523]

[198]. Harford CG, Hamlin A, Parker E. Electron microscopy of HeLa cells after the ingestion of colloidal gold. J. Biophys. Biochem. Cytol. 1957; 3:749–756. [PubMed: 13475389]

[199]. Dempsey EW, Wislocki GB. The use of silver nitrate as a vital stain, and its distribution in several mammalian tissues as studied with the electron microscope. J. Biophys. Biochem. Cytol. 1955; 1:111–118. [PubMed: 14381433]

[200]. Bessing C. Alternatives to high noble dental casting gold alloys type 3. An in vitro in vivo study. Swed. Dent. J. Suppl. 1988; 53:1–56. [PubMed: 3293245]

[201]. Pistorius A, Willershausen B. Biocompatibility of dental materials in two human cell lines. Eur. J. Med. Res. 2002; 7:81–88. [PubMed: 11891149]

[202]. Shukla R, Bansal V, Chaudhary M, Basu A, Bhonde RR, Sastry M. Biocompatibility of gold nanoparticles and their endocytotic fate inside the cellular compartment: a microscopic overview. Langmuir. 2005; 21:10644–10654. [PubMed: 16262332]

[203]. Hainfeld JF, Slatkin DN, Focella TM, Smilowitz HM. Gold nanoparticles: a new X-ray contrast agent. Br. J. Radiol. 2006; 79:248–253. [PubMed: 16498039]

[204]. Boote E, Fent G, Kattumuri V, Casteel S, Katti K, Chanda N, Kannan R, Churchill R. Gold nanoparticle contrast in a phantom and juvenile swine: models for molecular imaging of human organs using X-ray computed tomography. Acad. Radiol. 2010; 17:410–417. [PubMed: 20207313]

[205]. Oh MH, Lee N, Kim H, Park SP, Piao Y, Lee J, Jun SW, Moon WK, Choi SH, Hyeon T. Large-scale synthesis of bioinert tantalum oxide nanoparticles for X-ray computed tomography imaging and bimodal image-guided sentinel lymph node mapping. J. Am. Chem. Soc. 2011; 133:5508–5515. [PubMed: 21428437]

[206]. Bonitatibus PJ Jr. Torres AS, Goddard GD, FitzGerald PF, Kulkarni AM. Synthesis, characterization, and computed tomography imaging of a tantalum oxide nanoparticle imaging agent. Chem. Commun. (Camb.). 2010; 46:8956–8958. [PubMed: 20976321]

[207]. Reed MA, Randall JN, Aggarwal RJ, Matyi RJ, Moore TM, Wetsel AE. Observation of discrete electronic states in a zero-dimensional semiconductor nano-structure. Phys. Rev. Lett. 1988; 60:535–537. [PubMed: 10038575]

[208]. Akerman ME, Chan WC, Laakkonen P, Bhatia SN, Ruoslahti E. Nanocrystal targeting in vivo. Proc. Natl. Acad. Sci. U. S. A. 2002; 99:12617–12621. [PubMed: 12235356]

[209]. Smith AM, Wen MM, Nie S. Imaging dynamic cellular events with quantum dots: the bright future. Biochemistry (Lond). 2010; 32:12.

[210]. Zaman MB, Baral TN, Jakubek ZJ, Zhang J, Wu X, Lai E, Whitfield D, Yu K. Single-domain antibody bioconjugated near-IR quantum dots for targeted cellular imaging of pancreatic cancer. J. Nanosci. Nanotechnol. 2011; 11:3757–3763. [PubMed: 21780366]

[211]. Yang K, Zhao C, Cao YA, Tang H, Bai YL, Huang H, Zhao CR, Chen R, Zhao D. In vivo and in situ imaging of head and neck squamous cell carcinoma using near-infrared fluorescent quantum dot probes conjugated with epidermal growth factor receptor monoclonal antibodies in mice. Oncol. Rep. 2012

[212]. Sugiyama T, Kuroda S, Osanai T, Shichinohe H, Kuge Y, Ito M, Kawabori M, Iwasaki Y. Near-infrared fluorescence labeling allows noninvasive tracking of bone marrow stromal cells transplanted into rat infarct brain. Neurosurgery. 2011; 68:1036–1047. (discussion 1047). [PubMed: 21221028]

[213]. Kawabori M, Kuroda S, Sugiyama T, Ito M, Shichinohe H, Houkin K, Kuge Y, Tamaki N. Intracerebral, but not intravenous, transplantation of bone marrow stromal cells enhances functional recovery in rat cerebral infarct: an optical imaging study. Neuropathology. 2011

[214]. Yukawa H, Watanabe M, Kaji N, Okamoto Y, Tokeshi M, Miyamoto Y, Noguchi H, Baba Y, Hayashi S. Monitoring transplanted adipose tissue-derivedstem cells combined with heparin in the liver by fluorescence imaging using quantum dots. Biomaterials. 2012; 33:2177–2186. [PubMed: 22192539]

[215]. Rak-Raszewska A, Marcello M, Kenny S, Edgar D, See V, Murray P. Quantum dots do not affect the behaviour of mouse embryonic stem cells and kidney stem cells and are suitable for short-term tracking. PLoS One. 2012; 7:e32650. [PubMed: 22403689]

[216]. Ramot Y, Steiner M, Morad V, Leibovitch S, Amouyal N, Cesta MF, Nyska A. Pulmonary thrombosis in the mouse following intravenous administration of quantum dot-labeled mesenchymal cells. Nanotoxicology. 2010; 4:98–105. [PubMed: 20795905]

[217]. Wu C, Bull B, Szymanski C, Christensen K, McNeill J. Multicolor conjugated polymer dots for biological fluorescence imaging. ACS Nano. 2008; 2:2415–2423. [PubMed: 19206410]

[218]. Aoki H, Kakuta J, Yamaguchi T, Nitahara S, Ito S. Near-infrared fluorescent nanoparticle of low-bandgap p-conjugated polymer for in vivo molecular imaging. Polym. J. 2011; 43:937–940.

[219]. Reiss P, Couderc E, De Girolamo J, Pron A. Conjugated polymers/semiconductor nanocrystals hybrid materials—preparation, electrical transport properties and applications. Nanoscale. 2011; 3:446–489. [PubMed: 21152569]

[220]. Hu XB, Yue QH, Zhang XQ, Xu XQ, Wen Y, Chen YZ, Cheng XD, Yang L, Mu SJ. Hepatitis B virus genotypes and evolutionary profiles from blood donors from the northwest region of China. Virol. J. 2009; 6:199. [PubMed: 19917138]

[221]. Hui YY, Zhang B, Chang YC, Chang CC, Chang HC, Hsu JH, Chang K, Chang FH. Two-photon fluorescence correlation spectroscopy of lipid-encapsulated fluorescent nanodiamonds in living cells. Opt. Express. 2010; 18:5896–5905. [PubMed: 20389607]

[222]. Fudala R, Rout S, Maliwal BP, Zerda TW, Gryczynski I, Simanek E, Borejdo J, Rich R, Akopova I, Gryczynski Z. FRET enhanced fluorescent nanodiamonds. Curr. Pharm. Biotechnol. 2012

[223]. Schrand AM, Huang H, Carlson C, Schlager JJ, Sawa E. Omacr, Hussain SM, Dai L. Are diamond nanoparticles cytotoxic? J. Phys. Chem. B. 2007; 111:2–7. [PubMed: 17201422]

[224]. Vaijayanthimala V, Tzeng YK, Chang HC, Li CL. The biocompatibility of fluorescent nanodiamonds and their mechanism of cellular uptake. Nanotechnology. 2009; 20:425103. [PubMed: 19779240]

[225]. Xing Y, Xiong W, Zhu L, Osawa E, Hussin S, Dai L. DNA damage in embryonic stem cells caused by nanodiamonds. ACS Nano. 2011; 5:2376–2384. [PubMed: 21370893]

[226]. Hilderbrand SA, Shao F, Salthouse C, Mahmood U, Weissleder R. Upconverting luminescent nanomaterials: application to in vivo bioimaging. Chem. Commun. (Camb.). 2009:4188–4190. [PubMed: 19585016]

[227]. Zhou J, Liu Z, Li F. Upconversion nanophosphors for small-animal imaging. Chem. Soc. Rev. 2012; 41:1323–1349. [PubMed: 22008740]

[228]. Nagarajan S, Zhang Y. Upconversion fluorescent nanoparticles as a potential tool for in-depth imaging. Nanotechnology. 2011; 22:395101. [PubMed: 21891842]

[229]. Yang T, Sun Y, Liu Q, Feng W, Yang P, Li F. Cubic sub-20 nm NaLuF(4)-based upconversion nanophosphors for high-contrast bioimaging in different animal species. Biomaterials. 2012; 33:3733–3742. [PubMed: 22361097]

[230]. Carroll BA, Turner RJ, Tickner EG, Boyle DB, Young SW. Gelatin encapsulated nitrogen microbubbles as ultrasonic contrast agents. Invest. Radiol. 1980; 15:260–266. [PubMed: 7399850]

[231]. Gullace G, Savoia MT, Locatelli V, Ravizza PF, Ranzi C. Contrast echocardiography of the inferior vena cava. G. Ital. Cardiol. 1981; 11:2017–2026. [PubMed: 6213438]

[232]. Calliada F, Campani R, Bottinelli O, Bozzini A, Sommaruga MG. Ultrasound contrast agents: basic principles. Eur. J. Radiol. 1998; 27(Suppl. 2):S157–S160. [PubMed: 9652516]

[233]. Wang Y, Li X, Zhou Y, Huang P, Xu Y. Preparation of nanobubbles for ultrasound imaging and intracelluar drug delivery. Int. J. Pharm. 2010; 384:148–153. [PubMed: 19781609]

[234]. Hwang TL, Fang CL, Al-Suwayeh SA, Yang LJ, Fang JY. Activated human neutrophil response to perfluorocarbon nanobubbles: oxygen-dependent and -independent cytotoxic responses. Toxicol. Lett. 2011; 203:172–180. [PubMed: 21439357]

[235]. Kolivoska V, Gal M, Hromadova M, Lachmanova S, Tarabkova H, Janda P, Pospisil L, Turonova AM. Bovine serum albumin film as a template for controlled nanopancake and

nanobubble formation: In situ atomic force microscopy and nanolithography study. Colloids Surf. B Biointerfaces. 2012

[236]. Yin T, Wang P, Zheng R, Zheng B, Cheng D, Zhang X, Shuai X. Nanobubbles for enhanced ultrasound imaging of tumors. Int. J. Nanomedicine. 2012; 7:895–904. [PubMed: 22393289]

[237]. Di W, Ren X, Zhao H, Shirahata N, Sakka Y, Qin W. Single-phased luminescent mesoporous nanoparticles for simultaneous cell imaging and anticancer drug delivery. Biomaterials. 2011; 32:7226–7233. [PubMed: 21745687]

[238]. Jia G, Zhang C, Ding S, Wang L. General synthesis route to fabricate uniform upconversion luminescent gadolinium oxide hollow spheres. J. Nanosci. Nanotechnol. 2011; 11:6875–6879. [PubMed: 22103093]

[239]. Lu LT, Tung LD, Robinson I, Ung D, Tan B, Long J, Cooper AI, Fernig DG, Thanh NT. Size and shape control for water-soluble magnetic cobalt nanoparticles using polymer ligands. J. Mater. Chem. 2008; 18:2453–2458.

[240]. Lu LT, Tung le D, Long J, Fernig DG, Thanh NT. Facile synthesis of stable, water-soluble magnetic CoPt hollow nanostructures assisted by multi-thiol ligands. J. Mater. Chem. 2009; 19:6023–6028.

[241]. Meng X, Seton HC, Lu le T, Prior IA, Thanh NT, Song B. Magnetic CoPt nanoparticles as MRI contrast agent for transplanted neural stem cells detection. Nanoscale. 2011; 3:977–984. [PubMed: 21293831]

[242]. Wan H, Shi S, Bai L, Shamsuzzoha M, Harrell JW, Street SC. Synthesis and characterization of CoPt nanoparticles prepared by room temperature chemical reduction with PAMAM dendrimer as template. J. Nanosci. Nanotechnol. 2010; 10:5089–5092. [PubMed: 21125854]

[243]. Lappalainen RS, Narkilahti S, Huhtala T, Liimatainen T, Suuronen T, Narvanen A, Suuronen R, Hovatta O, Jolkkonen J. The SPECT imaging shows the accumulation of neural progenitor cells into internal organs after systemic administration in middle cerebral artery occlusion rats. Neurosci. Lett. 2008; 440:246–250. [PubMed: 18572314]

[244]. Wong RM, Gilbert DA, Liu K, Louie AY. Rapid size-controlled synthesis of dextran-coated, 64Cu-doped iron oxide nanoparticles. ACS Nano. 2012

[245]. Xing Z, Wang J, Ke H, Zhao B, Yue X, Dai Z, Liu J. The fabrication of novel nanobubble ultrasound contrast agent for potential tumor imaging. Nanotechnology. 2010; 21:145607. [PubMed: 20220227]

[246]. Salehizadeh H, Hekmatian E, Sadeghi M, Kennedy K. Synthesis and characterization of core-shell FeO–gold–chitosan nanostructure. J. Nanobiotechnol. 2012; 10:3.

[247]. Arifin DR, Bulte JW. Imaging of pancreatic islet cells. Diabetes Metab. Res. Rev. 2011; 27:761–766. [PubMed: 22069256]

[248]. Winter PM, Cai K, Chen J, Adair CR, Kiefer GE, Athey PS, Gaffney PJ, Buff CE, Robertson JD, Caruthers SD, Wickline SA, Lanza GM. Targeted PARACEST nanoparticle contrast agent for the detection of fibrin. Magn. Reson. Med. 2006; 56:1384–1388. [PubMed: 17089356]

[249]. Hsiao JK, Tsai CP, Chung TH, Hung Y, Yao M, Liu HM, Mou CY, Yang CS, Chen YC, Huang DM. Mesoporous silica nanoparticles as a delivery system of gadolinium for effective human stem cell tracking. Small. 2008; 4:1445–1452. [PubMed: 18680095]

[250]. Vuu K, Xie J, McDonald MA, Bernardo M, Hunter F, Zhang Y, Li K, Bednarski M, Guccione S. Gadolinium–rhodamine nanoparticles for cell labeling and tracking via magnetic resonance and optical imaging. Bioconjug. Chem. 2005; 16:995–999. [PubMed: 16029042]

[251]. Kim HM, Lee H, Hong KS, Cho MY, Sung MH, Poo H, Lim YT. Synthesis and high performance of magnetofluorescent polyelectrolyte nanocomposites as MR/near-infrared multimodal cellular imaging nanoprobes. ACS Nano. 2011; 5:8230–8240. [PubMed: 21932788]

[252]. Cha EJ, Jang ES, Sun IC, Lee IJ, Ko JH, Kim YI, Kwon IC, Kim K, Ahn CH. Development of MRI/NIRF ‘activatable’ multimodal imaging probe based on iron oxide nanoparticles. J. Control. Release. 2011; 155:152–158. [PubMed: 21801769]

[253]. Lee CM, Jang D, Kim J, Cheong SJ, Kim EM, Jeong MH, Kim SH, Kim DW, Lim ST, Sohn MH, Jeong YY, Jeong HJ. Oleyl-chitosan nanoparticles based on a dual probe for optical/MR imaging in vivo. Bioconjug. Chem. 2011; 22:186–192. [PubMed: 21243999]

[254]. Xu H, Regino CA, Koyama Y, Hama Y, Gunn AJ, Bernardo M, Kobayashi H, Choyke PL, Brechbiel MW. Preparation and preliminary evaluation of a biotin-targeted, lectin-targeted dendrimer-based probe for dual-modality magnetic resonance and fluorescence imaging. Bioconjug. Chem. 2007; 18:1474–1482. [PubMed: 17711320]

[255]. van Schooneveld MM, Cormode DP, Koole R, van Wijngaarden JT, Calcagno C, Skajaa T, Hilhorst J, Hart D.C. t, Fayad ZA, Mulder WJ, Meijerink A. A fluorescent, paramagnetic and PEGylated gold/silica nanoparticle for MRI, CT and fluorescence imaging. Contrast Media Mol. Imaging. 2010; 5:231–236. [PubMed: 20812290]

[256]. Filonov GS, Piatkevich KD, Ting LM, Zhang J, Kim K, Verkhusha VV. Bright and stable near-infrared fluorescent protein for in vivo imaging. Nat. Biotechnol. 2011; 29:757–761. [PubMed: 21765402]

[257]. Jacobs A, Voges J, Reszka R, Lercher M, Gossmann A, Kracht L, Kaestle C, Wagner R, Wienhard K, Heiss WD. Positron-emission tomography of vector-mediated gene expression in gene therapy for gliomas. Lancet. 2001; 358:727–729. [PubMed: 11551583]

[258]. Reszka RC, Jacobs A, Voges J. Liposome-mediated suicide gene therapy in humans. Methods Enzymol. 2005; 391:200–208. [PubMed: 15721383]

[259]. Yaghoubi SS, Jensen MC, Satyamurthy N, Budhiraja S, Paik D, Czernin J, Gambhir SS. Noninvasive detection of therapeutic cytolytic T cells with 18F-FHBG PET in a patient with glioma. Nat. Clin. Pract. Oncol. 2009; 6:53–58. [PubMed: 19015650]

[260]. Gonzalez-McQuire R, Green DW, Partridge KA, Oreffo RO, Mann S, Davis SA. Coating of human mesenchymal cells in 3D culture with bioinorganic nanoparticles promotes osteoblastic differentiation and gene transfection. Adv. Mater. 2007; 19:2236–2240.

[261]. Hsu SH, Ho TT, Tseng TC. Nanoparticle uptake and gene transfer efficiency for MSCs on chitosan and chitosan-hyaluronan substrates. Biomaterials. 2012; 33:3639–3650. [PubMed: 22364729]

[262]. Date I, Miyoshi Y, Ono T, Imaoka T, Furuta T, Asari S, Ohmoto T, Iwata H. Preliminary report of polymer-encapsulated dopamine-secreting cell grafting into the brain. Cell Transplant. 1996; 5:S17–S19. [PubMed: 8889222]

[263]. Lim F, Moss RD. Microencapsulation of living cells and tissues. J. Pharm. Sci. 1981; 70:351–354. [PubMed: 7014829]

[264]. Barnett BP, Arepally A, Karmarkar PV, Qian D, Gilson WD, Walczak P, Howland V, Lawler L, Lauzon C, Stuber M, Kraitchman DL, Bulte JW. Magnetic resonance-guided, real-time targeted delivery and imaging of magnetocapsules immunoprotecting pancreatic islet cells. Nat. Med. 2007; 13:986–991. [PubMed: 17660829]

[265]. Link TW, Woodrum D, Gilson WD, Pan L, Qian D, Kraitchman DL, Bulte JW, Arepally A, Weiss CR. MR-guided portal vein delivery and monitoring of magnetocapsules: assessment of physiologic effects on the liver. J. Vasc. Interv. Radiol. 2011; 22:1335–1340. [PubMed: 21816623]

[266]. Mills PH, Hitchens TK, Foley LM, Link T, Ye Q, Weiss CR, Thompson JD, Gilson WD, Arepally A, Melick JA, Kochanek PM, Ho C, Bulte JW, Ahrens ET. Automated detection and characterization of SPIO-labeled cells and capsules using magnetic field perturbations. Magn. Reson. Med. 2012; 67:278–289. [PubMed: 21656554]

[267]. Barnett BP, Kraitchman DL, Lauzon C, Magee CA, Walczak P, Gilson WD, Arepally A, Bulte JW. Radiopaque alginate microcapsules for X-ray visualization and immunoprotection of cellular therapeutics. Mol. Pharm. 2006; 3:531–538. [PubMed: 17009852]

[268]. Kedziorek DA, Hofmann LV, Fu Y, Gilson WD, Cosby KM, Kohl B III, Barnett BP, Simons BW, Walczak P, Bulte JW, Gabrielson K, Kraitchman DL. X-ray-visible microcapsules containing mesenchymal stem cells improve hindlimb perfusion in a rabbit model of peripheral arterial disease. Stem Cells. 2012

[269]. Arifin DR, Manek S, Call E, Arepally A, Bulte JW. Microcapsules with intrinsic barium radiopacity for immunoprotection and X-ray/CT imaging of pancreatic islet cells. Biomaterials. 2012; 33:4681–4689. [PubMed: 22444642]

[270]. Arifin DR, Long CM, Gilad AA, Alric C, Roux S, Tillement O, Link TW, Arepally A, Bulte JW. Trimodal gadolinium-gold microcapsules containing pancreatic islet cells restore

normoglycemia in diabetic mice and can be tracked by using US, CT, and positive-contrast MR imaging. Radiology. 2011; 260:790–798. [PubMed: 21734156]

[271]. Barnett BP, Arepally A, Stuber M, Arifin DR, Kraitchman DL, Bulte JW. Synthesis of magnetic resonance-, X-ray- and ultrasound-visible alginate microcapsules for immunoisolation and noninvasive imaging of cellular therapeutics. Nat. Protoc. 2011; 6:1142–1151. [PubMed: 21799484]

[272]. Kim J, Arifin DR, Muja N, Kim T, Gilad AA, Kim H, Arepally A, Hyeon T, Bulte JW. Multifunctional capsule-in-capsules for immunoprotection and trimodal imaging. Angew. Chem. Int. Ed Engl. 2011; 50:2317–2321. [PubMed: 21351344]

[273]. Barnett BP, Ruiz-Cabello J, Hota P, Liddell R, Walczak P, Howland V, Chacko VP, Kraitchman DL, Arepally A, Bulte JW. Fluorocapsules for improved function, immunoprotection, and visualization of cellular therapeutics with MR, US, and CT imaging. Radiology. 2011; 258:182–191. [PubMed: 20971778]

[274]. Shen F, Li AA, Gong YK, Somers S, Potter MA, Winnik FM, Chang PL. Encapsulation of recombinant cells with a novel magnetized alginate for magnetic resonance imaging. Hum. Gene Ther. 2005; 16:971–984. [PubMed: 16076255]

[275]. Foltz WD, Ormiston ML, Stewart DJ, Courtman DW, Dick AJ. MRI characterization of agarose gel micro-droplets at acute time-points within the rabbit lumbar muscle. Biomaterials. 2008; 29:1844–1852. [PubMed: 18206227]

[276]. Miura S, Teramura Y, Iwata H. Encapsulation of islets with ultra-thin polyion complex membrane through poly(ethylene glycol)-phospholipids anchored to cell membrane. Biomaterials. 2006; 27:5828–5835. [PubMed: 16919725]

[277]. Tatsumi K, Ohashi K, Teramura Y, Utoh R, Kanegae K, Watanabe N, Mukobata S, Nakayama M, Iwata H, Okano T. The non-invasive cell surface modification of hepatocytes with PEG-lipid derivatives. Biomaterials. 2012; 33:821–828. [PubMed: 22027599]

[278]. Zhi ZL, Liu B, Jones PM, Pickup JC. Polysaccharide multilayer nanoencapsulation of insulin-producing beta-cells grown as pseudoislets for potential cellular delivery of insulin. Biomacromolecules. 2010; 11:610–616. [PubMed: 20108955]

[279]. Bible E, Dell'Acqua F, Solanky B, Balducci A, Crapo PM, Badylak SF, Ahrens ET, Modo M. Non-invasive imaging of transplanted human neural stem cells and ECM scaffold remodeling in the stroke-damaged rat brain by (19)F- and diffusion-MRI. Biomaterials. 2012; 33:2858–2871. [PubMed: 22244696]

[280]. Terrovitis JV, Bulte JW, Sarvananthan S, Crowe LA, Sarathchandra P, Batten P, Sachlos E, Chester AH, Czernuszka JT, Firmin DN, Taylor PM, Yacoub MH. Magnetic resonance imaging of ferumoxide-labeled mesenchymal stem cells seeded on collagen scaffolds-relevance to tissue engineering. Tissue Eng. 2006; 12:2765–2775. [PubMed: 17518646]

[281]. Henriksson HB, Svanvik T, Jonsson M, Hagman M, Horn M, Lindahl A, Brisby H. Transplantation of human mesenchymal stems cells into intervertebral discs in a xenogeneic porcine model. Spine (Phila Pa 1976). 2009; 34:141–148. [PubMed: 19112334]

[282]. Gao J, Liu R, Wu J, Liu Z, Li J, Zhou J, Hao T, Wang Y, Du Z, Duan C, Wang C. The use of chitosan based hydrogel for enhancing the therapeutic benefits of adipose-derived MSCs for acute kidney injury. Biomaterials. 2012; 33:3673–3681. [PubMed: 22361096]

[283]. Cheng K, Shen D, Smith J, Galang G, Sun B, Zhang J, Marban E. Transplantation of platelet gel spiked with cardiosphere-derived cells boosts structural and functional benefits relative to gel transplantation alone in rats with myocardial infarction. Biomaterials. 2012; 33:2872–2879. [PubMed: 22243801]

[284]. Yang Y, de Gervai P. Dreessen, Sun J, Glogowski M, Gussakovsky E, Kupriyanov V. MRI studies of cryoinjury infarction in pig hearts: ii. Effects of intrapericardial delivery of adipose-derived stem cells (ADSC) embedded in agarose gel. NMR Biomed. 2012; 25:227–235. [PubMed: 21774011]

[285]. Bencherif SA, Siegwart DJ, Srinivasan A, Horkay F, Hollinger JO, Washburn NR, Matyjaszewski K. Nanostructured hybrid hydrogels prepared by a combination of atom transfer radical polymerization and free radical polymerization. Biomaterials. 2009; 30:5270–5278. [PubMed: 19592087]

[286]. Zhu H, Li Y, Qiu R, Shi L, Wu W, Zhou S. Responsive fluorescent Bi(2)O(3) @PVA hybrid nanogels for temperature-sensing, dual-modal imaging, and drug delivery. Biomaterials. 2012; 33:3058–3069. [PubMed: 22257723]

[287]. Rejinold NS, Chennazhi KP, Tamura H, Nair SV, Rangasamy J. Multifunctional chitin nanogels for simultaneous drug delivery, bioimaging, and biosensing. ACS Appl. Mater. Interfaces. 2011; 3:3654–3665. [PubMed: 21863797]

[288]. Gong Y, Fan M, Gao F, Hong J, Liu S, Luo S, Yu J, Huang J. Preparation and characterization of amino-functionalized magnetic nanogels via photopolymerization for MRI applications. Colloids Surf. B Biointerfaces. 2009; 71:243–247. [PubMed: 19278838]

[289]. Toita S, Hasegawa U, Koga H, Sekiya I, Muneta T, Akiyoshi K. Protein-conjugated quantum dots effectively delivered into living cells by a cationic nanogel. J. Nanosci. Nanotechnol. 2008; 8:2279–2285. [PubMed: 18572638]

[290]. Hasegawa U, Nomura SM, Kaul SC, Hirano T, Akiyoshi K. Nanogel-quantum dot hybrid nanoparticles for live cell imaging. Biochem. Biophys. Res. Commun. 2005; 331:917–921. [PubMed: 15882965]

[291]. Siegwart DJ, Srinivasan A, Bencherif SA, Karunanidhi A, Oh JK, Vaidya S, Jin R, Hollinger JO, Matyjaszewski K. Cellular uptake of functional nanogels prepared by inverse miniemulsion ATRP with encapsulated proteins, carbohydrates, and gold nanoparticles. Biomacromolecules. 2009; 10:2300–2309. [PubMed: 19572639]

[292]. Rago G, Bauer B, Svedberg F, Gunnarsson L, Ericson MB, Bonn M, Enejder A. Uptake of gold nanoparticles in healthy and tumor cells visualized by nonlinear optical microscopy. J. Phys. Chem. B. 2011; 115:5008–5016. [PubMed: 21469683]

[293]. Rago G, Langer CM, Brackman C, Day JP, Domke KF, Raschzok N, Schmidt C, Sauer IM, Enejder A, Mogl MT, Bonn M. CARS microscopy for the visualization of micrometer-sized iron oxide MRI contrast agents in living cells. Biomed. Opt. Express. 2011; 2:2470–2483. [PubMed: 21991541]

[294]. Moger J, Johnston BD, Tyler CR. Imaging metal oxide nanoparticles in biological structures with CARS microscopy. Opt. Express. 2008; 16:3408–3419. [PubMed: 18542432]

[295]. Saar BG, Freudiger CW, Reichman J, Stanley CM, Holtom GR, Xie XS. Video-rate molecular imaging in vivo with stimulated Raman scattering. Science. 2010; 330:1368–1370. [PubMed: 21127249]

[296]. Ando J, Fujita K, Smith NI, Kawata S. Dynamic SERS imaging of cellular transport pathways with endocytosed gold nanoparticles. Nano Lett. 2011; 11:5344–5348. [PubMed: 22059676]

[297]. McColgan P, Sharma P, Bentley P. Stem cell tracking in human trials: a meta-regression. Stem Cell Rev. 2011; 7:1031–1040. [PubMed: 21475954]

[298]. Callera F, de Melo CM. Magnetic resonance tracking of magnetically labeled autologous bone marrow CD34+ cells transplanted into the spinal cord via lumbar puncture technique in patients with chronic spinal cord injury: CD34+ cells' migration into the injured site. Stem Cells Dev. 2007; 16:461–466. [PubMed: 17610376]

[299]. Toso C, Vallee JP, Morel P, Ris F, Demuylder-Mischler S, Lepetit-Coiffe M, Marangon N, Saudek F, Shapiro A.M. James, Bosco D, Berney T. Clinical magnetic resonance imaging of pancreatic islet grafts after iron nanoparticle labeling. Am. J. Transplant. 2008; 8:701–706. [PubMed: 18294167]

[300]. Karussis D, Karageorgiou C, Vaknin-Dembinsky A, Gowda-Kurkalli B, Gomori JM, Kassis I, Bulte JW, Petrou P, Ben-Hur T, Abramsky O, Slavin S. Safety and immunological effects of mesenchymal stem cell transplantation in patients with multiple sclerosis and amyotrophic lateral sclerosis. Arch. Neurol. 2010; 67:1187–1194. [PubMed: 20937945]

[301]. Jozwiak S, Habich A, Kotulska K, Sarnowska A, Kropiwnicki T, Janowski M, Jurkiewicz E, Lukomska B, Kmiec T, Walecki J, Roszkowski M, Litwin M, Oldak T, Boruczkowski D, Domanska-Janik K. Intracerebrobentricular transplantation of cord blood-derived neural progenitors in a child with severe global brain ischemic injury. Cell Med. 2010; 1:71–80.

[302]. Gulati N, Gupta H. Two faces of carbon nanotube: toxicities and pharmaceutical applications. Crit. Rev. Ther. Drug Carrier Syst. 2012; 29:65–88. [PubMed: 22356722]

[303]. Park MV, Neigh AM, Vermeulen JP, de la Fonteyne LJ, Verharen HW, Briede JJ, van Loveren H, de Jong WH. The effect of particle size on the cytotoxicity, inflammation, developmental toxicity and genotoxicity of silver nanoparticles. Biomaterials. 2011; 32:9810–9817. [PubMed: 21944826]

[304]. Yang B, Wang Q, Lei R, Wu C, Shi C, Yuan Y, Wang Y, Luo Y, Hu Z, Ma H, Liao M. Systems toxicology used in nanotoxicology: mechanistic insights into the hepatotoxicity of nano-copper particles from toxicogenomics. J. Nanosci. Nanotechnol. 2010; 10:8527–8537. [PubMed: 21121362]

[305]. Prabhu BM, Ali SF, Murdock RC, Hussain SM, Srivatsan M. Copper nanoparticles exert size and concentration dependent toxicity on somatosensory neurons of rat. Nanotoxicology. 2010; 4:150–160. [PubMed: 20543894]

[306]. Chen YS, Hung YC, Lin LW, Liau I, Hong MY, Huang GS. Size-dependent impairment of cognition in mice caused by the injection of gold nanoparticles. Nanotechnology. 2010; 21:485102. [PubMed: 21051801]

[307]. Zandberg WF, Bakhtiari AB, Erno Z, Hsiao D, Gates BD, Claydon T, Branda NR. Photothermal release of small molecules from gold nanoparticles in live cells. Nanomedicine. 2011

[308]. Pelicci PG, Dalton P, Orecchia R. Heating cancer stem cells to reduce tumor relapse. Breast Cancer Res. 2011; 13:305. [PubMed: 21575278]

[309]. Tamariz E, Wan AC, Pek YS, Giordano M, Hernandez-Padron G, Varela-Echavarria A, Velasco I, Castano VM. Delivery of chemotropic proteins and improvement of dopaminergic neuron outgrowth through a thixotropic hybrid nano-gel. J. Mater. Sci. Mater. Med. 2011; 22:2097–2109. [PubMed: 21744103]

[310]. Bulte JW, Kostura L, Mackay A, Karmarkar PV, Izbudak I, Atalar E, Fritzges D, Rodriguez ER, Young RG, Marcelino M, Pittenger MF, Kraitchman DL. Feridex-labeled mesenchymal stem cells: cellular differentiation and MR assessment in a canine myocardial infarction model. Acad. Radiol. 2005; 12(Suppl. 1):S2–S6. [PubMed: 16106536]

[311]. Kostura L, Kraitchman DL, Mackay AM, Pittenger MF, Bulte JW. Feridex labeling of mesenchymal stem cells inhibits chondrogenesis but not adipogenesis or osteogenesis. NMR Biomed. 2004; 17:513–517. [PubMed: 15526348]

[312]. Berman, S.M. Cromer; Kshitiz; Wang, CJ.; Orukari, I.; Levchenko, A.; Bulte, JW.; Walczak, P. Cell motility of neural stem cells is reduced after SPIO-labeling, which is mitigated after exocytosis. Magn. Reson. Med. 2012

[313]. Lepore AC, Walczak P, Rao MS, Fischer I, Bulte JW. MR imaging of lineage-restricted neural precursors following transplantation into the adult spinal cord. Exp. Neurol. 2006; 201:49–59. [PubMed: 16764862]

[314]. Silva AK, Wilhelm C, Kolosnjaj-Tabi J, Luciani N, Gazeau F. Cellular transfer of magnetic nanoparticles via cell microvesicles: impact on cell tracking by magnetic resonance imaging. Pharm. Res. 2012

[315]. Lammers T, Kiessling F, Hennink WE, Storm G. Nanotheranostics and image-guided drug delivery: current concepts and future directions. Mol. Pharm. 2010; 7:1899–1912. [PubMed: 20822168]

[316]. Narayanan S, Sathy BN, Mony U, Koyakutty M, Nair SV, Menon D. Biocompatible magnetite/gold nanohybrid contrast agents via green chemistry for MRI and CT bioimaging. ACS Appl. Mater. Interfaces. 2012; 4:251–260. [PubMed: 22103574]

[317]. Mackay PS, Kremers GJ, Kobukai S, Cobb JG, Kuley A, Rosenthal SJ, Koktysh DS, Gore JC, Pham W. Multimodal imaging of dendritic cells using a novel hybrid magneto-optical nanoprobe. Nanomedicine. 2011; 7:489–496. [PubMed: 21215329]

[318]. Patel D, Kell A, Simard B, Xiang B, Lin HY, Tian G. The cell labeling efficacy, cytotoxicity and relaxivity of copper-activated MRI/PET imaging contrast agents. Biomaterials. 2011; 32:1167–1176. [PubMed: 21035183]

[319]. Madru R, Kjellman P, Olsson F, Wingardh K, Ingvar C, Stahlberg F, Olsrud J, Latt J, Fredriksson S, Knutsson L, Strand SE. 99mTc-Labeled superparamagnetic iron oxide nanoparticles for multimodality SPECT/MRI of sentinel lymph nodes. J. Nucl. Med. 2012; 53:459–463. [PubMed: 22323777]

[320]. Martin de Rosales, R. Torres; Tavare, R.; Glaria, A.; Varma, G.; Protti, A.; Blower, PJ. (m)Tc-bisphosphonate–iron oxide nanoparticle conjugates for dual-modality biomedical imaging. Bioconjug. Chem. 2011; 22:455–465. [PubMed: 21338098]

[321]. Kryza D, Taleb J, Janier M, Marmuse L, Miladi I, Bonazza P, Louis C, Perriat P, Roux S, Tillement O, Billotey C. Biodistribution study of nanometric hybrid gadolinium oxide particles as a multimodal SPECT/MR/optical imaging and theragnostic agent. Bioconjug. Chem. 2011; 22:1145–1152. [PubMed: 21545181]

[322]. Fizet J, Riviere C, Bridot JL, Charvet N, Louis C, Billotey C, Raccurt M, Morel G, Roux S, Perriat P, Tillement O. Multi-luminescent hybrid gadolinium oxide nanoparticles as potential cell labeling. J. Nanosci. Nanotechnol. 2009; 9:5717–5725. [PubMed: 19908443]

[323]. Ha TL, Kim HJ, Shin J, Im GH, Lee JW, Heo H, Yang J, Kang CM, Choe YS, Lee JH, Lee IS. Development of target-specific multimodality imaging agent by using hollow manganese oxide nanoparticles as a platform. Chem. Commun. (Camb.). 2011; 47:9176–9178. [PubMed: 21761053]

[324]. Luo T, Huang P, Gao G, Shen G, Fu S, Cui D, Zhou C, Ren Q. Mesoporous silica-coated gold nanorods with embedded indocyanine green for dual mode X-ray CT and NIR fluorescence imaging. Opt. Express. 2011; 19:17030–17039. [PubMed: 21935063]

[325]. Sun H, Yuan Q, Zhang B, Ai K, Zhang P, Lu L. Gd(III) functionalized gold nanorods for multimodal imaging applications. Nanoscale. 2011; 3:1990–1996. [PubMed: 21384042]

[326]. Park JA, Kim HK, Kim JH, Jeong SW, Jung JC, Lee GH, Lee J, Chang Y, Kim TJ. Gold nanoparticles functionalized by gadolinium–DTPA conjugate of cysteine as a multimodal bioimaging agent. Bioorg. Med. Chem. Lett. 2010; 20:2287–2291. [PubMed: 20188545]

[327]. Guerrero RS, Herance JR, Rojas S, Mena JF, Gispert JD, Acosta GA, Albericio F, Kogan MJ. Synthesis and in vivo evaluation of the biodistribution of a (18)f-labeled conjugate gold-nanoparticle-Peptide with potential biomedical application. Bioconjug. Chem. 2012; 23:399–408. [PubMed: 22284226]

[328]. Morales-Avila E, Ferro-Flores G, Ocampo-Garcia BE, De Leon-Rodriguez LM, Santos-Cuevas CL, Garcia-Becerra R, Medina LA, Gomez-Olivan L. Multimeric system of 99mTc-labeled gold nanoparticles conjugated to c[RGDfK(C)] for molecular imaging of tumor alpha(v)beta(3) expression. Bioconjug. Chem. 2011; 22:913–922. [PubMed: 21513349]

[329]. Xia A, Gao Y, Zhou J, Li C, Yang T, Wu D, Wu L, Li F. Core-shell NaYF4:Yb3+, Tm3+@FexOy nanocrystals for dual-modality T2-enhanced magnetic resonance and NIR-to-NIR upconversion luminescent imaging of small-animal lymphatic node. Biomaterials. 2011; 32:7200–7208. [PubMed: 21742376]

[330]. Zhou J, Yu M, Sun Y, Zhang X, Zhu X, Wu Z, Wu D, Li F. Fluorine-18-labeled Gd3+/Yb3+/Er3+ co-doped NaYF4 nanophosphors for multimodality PET/MR/ UCL imaging. Biomaterials. 2011; 32:1148–1156. [PubMed: 20965563]

[331]. Bakalova R, Zhelev Z, Kokuryo D, Spasov L, Aoki I, Saga T. Chemical nature and structure of organic coating of quantum dots is crucial for their application in imaging diagnostics. Int. J. Nanomedicine. 2011; 6:1719–1732. [PubMed: 21980235]

[332]. Stasiuk GJ, Tamang S, Imbert D, Poillot C, Giardiello M, Tisseyre C, Barbier EL, Fries PH, de Waard M, Reiss P, Mazzanti M. Cell-permeable Ln(III) chelate-functionalized InP quantum dots as multimodal imaging agents. ACS Nano. 2011; 5:8193–8201. [PubMed: 21888430]

[333]. Rosenberg JT, Kogot JM, Lovingood DD, Strouse GF, Grant SC. Intracellular bimodal nanoparticles based on quantum dots for high-field MRI at 21.1 T. Magn. Reson. Med. 2010; 64:871–882. [PubMed: 20575090]

[334]. Tu C, Ma X, House A, Kauzlarich SM, Louie AY. PET imaging and biodistribution of silicon quantum dots in mice. ACS Med. Chem. Lett. 2011; 2:285–288. [PubMed: 21546997]

[335]. Xu H, Cheng L, Wang C, Ma X, Li Y, Liu Z. Polymer encapsulated upconversion nanoparticle/iron oxide nanocomposites for multimodal imaging and magnetic targeted drug delivery. Biomaterials. 2011; 32:9364–9373. [PubMed: 21880364]

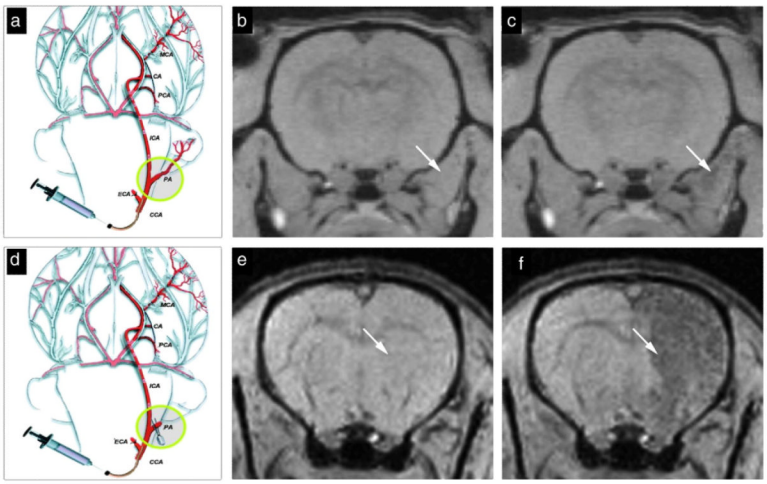

Fig. 1.

Real-time MR monitoring of injection accuracy. Following ligation of the external carotid and occipital arteries, the common carotid artery was cannulated (a) and SPIO-labeled cells were infused. In this experiment, the pterygopalatine artery was left intact. MR images were acquired immediately pre-injection (b) and post-injection (c). MR images demonstrate that the vast majority of cells localized into the extracerebral tissue, with negligible binding within the brain. When the pterygopalatine artery was ligated (d), all infused cells were perfused into the internal carotid artery and localized successfully into the ipsilateral hemisphere. Shown are the MR images acquired immediately before (e) and after injection (f). Reproduced, with permission, from Ref. [113].

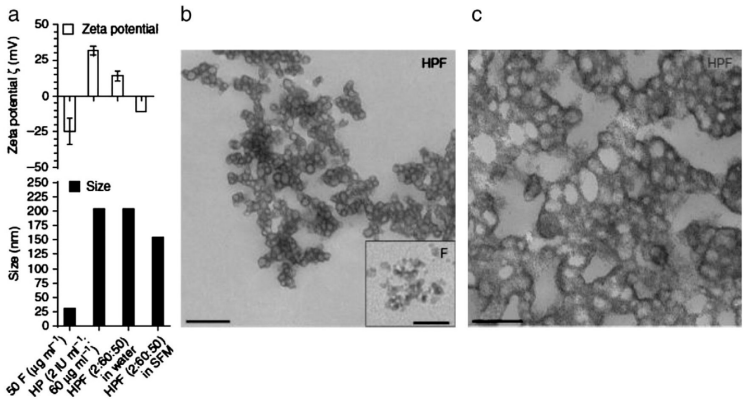

Fig. 2.

Characteristics of self-assembling heparin (H), protamine (P), and ferumoxytol (F) nanocomplexes (HPFs). (a) Graphs of the zeta potential (ζ) (top) and the particle size (bottom) of HPF nanocomplexes at a ratio of 2 IU ml^{-1} heparin: 60 μg ml^{-1} protamine: 50 μg ml^{-1} Feraheme® in sterile water and serum-free medium (SFM). Data are shown as mean±s.d. (b) HPF nanocomplexes formed by combining 2 IU ml^{-1} heparin: 60 μg ml^{-1} protamine: 50 μg ml^{-1} Feraheme® in sterile water, as observed by TEM. Scale bar, 0.6 μm. Inset, native Feraheme® nanoparticles. Scale bar, 20 nm. (c) HPFs at higher magnification. Scale bar, 0.3 μm. Reproduced, with permission, from Ref. [143].

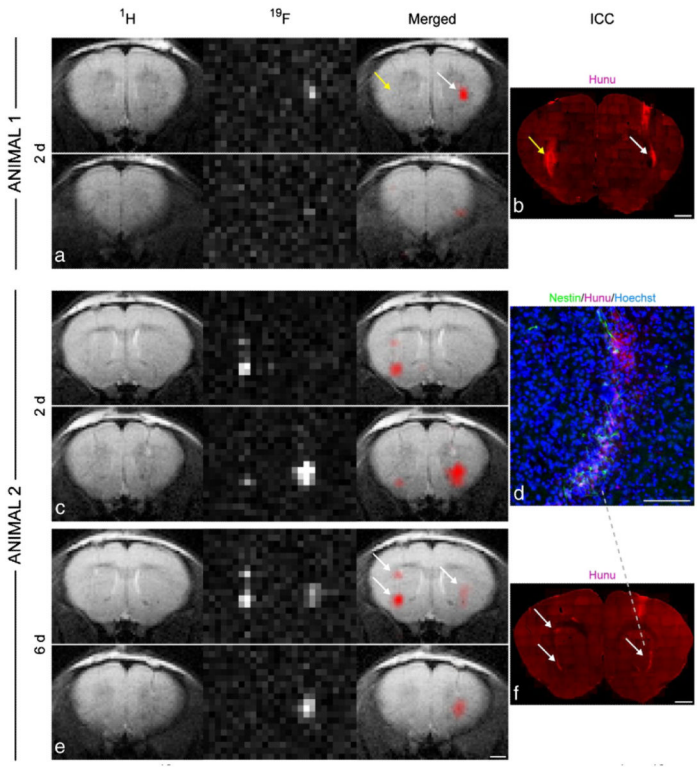

Fig. 3.

In vivo ^{19}F MRI and correlation with immunohistochemistry. ^{1}H, ^{19}F, and merged MR images of a mouse (animal 1), which had been injected with non-labeled control cells into the left striatum and labeled NSCs into the right hemisphere (a). Only the labeled cells generated a ^{19}F signal, whereas anti-human nuclear antigen (Hunu) staining confirmed the presence of cell grafts on both sides, indicated by the arrows (b). MRI of another mouse (animal 2) two days (c) and six days (e) after grafting showed no major signal loss in the ^{19}F images over time. This animal had received two deposits of labeled cells in the left striatum and one deposit in the right striatum. The location and intensity of ^{19}F signal from cell clusters, marked with white arrows, correlated well with anti-Hunu staining on histological sections. Note that the ^{19}F resolution allows the distinction of the two clusters in the left hemisphere (b, f). Only cells that were clearly immunoreactive to HuNu were considered as grafted human NSCs (d). Scale bars are 50 mm for d, 1 mm for all others. Reproduced, with permission, from Ref. [192].

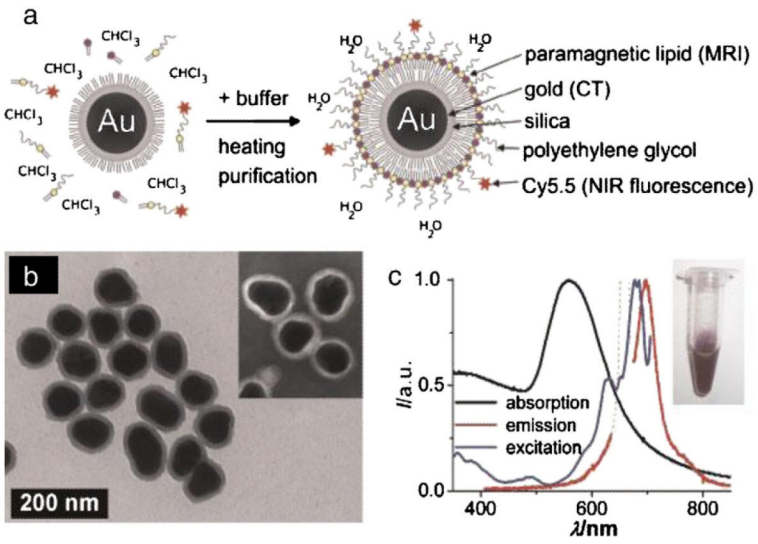

Fig. 4.

(a) Schematic representation of the nanoparticle lipid-coating procedure. (b) TEM image of hydrophobic gold/silica particles (88±9 nm). The inset shows a negative stain TEM image of the lipid-coated particles. (c) Absorption (black), emission (lexc 660 nm; red), and excitation (lem 710 nm; blue) spectra of the aqueous lipid-coated gold/silica particle dispersion (inset). Note that the dotted line in the emission spectrum is due to scattered excitation light, and thus, not attributable to Cy5.5 emission. Reproduced, with permission, from Ref. [255]. (For interpretation of the references to color in this figure legend, the reader is referred to the web version of this article.)

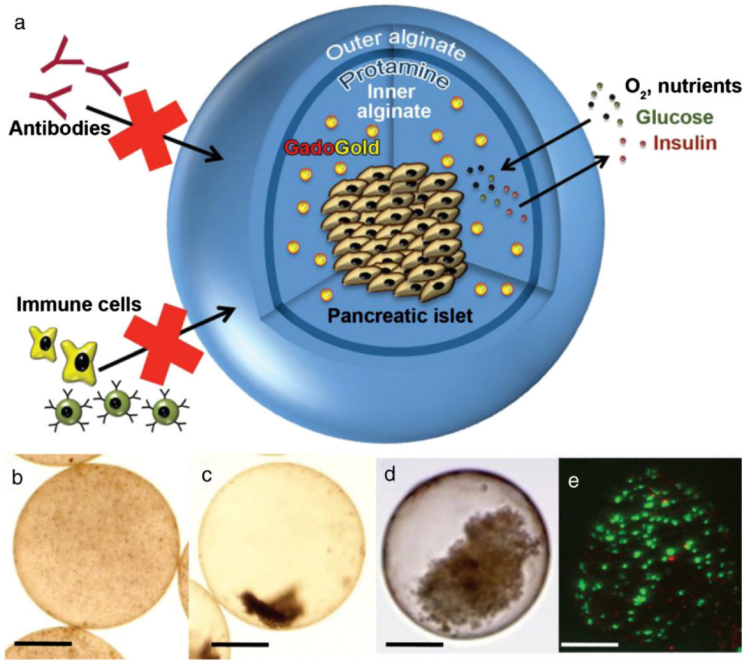

Fig. 5.

(a) Three-dimensional scheme of alginate-protamine sulfate-alginate (APSA) microcapsule containing GadoGold (GG). The semi-permeable microcapsule allows diffusion of oxygen, nutrients, glucose, and insulin, while the passage of immune cells and antibodies is blocked. (b ,c) Light microscopic images of the APSA-GG microcapsule 1 h (b) and two days (c) after synthesis. (d) Human pancreatic islet inside the APSA-GG microcapsule. (e) Fluorescence microscopic image shows viability staining of mouse insulinoma β-TC-6 cells inside the APSA-GG microcapsule. Green (fluorescein diacetate stain)=live cells, red (propidium iodide stain)=dead cells. Scale bars=200 mm. Reproduced, with permission, from Ref. [270].

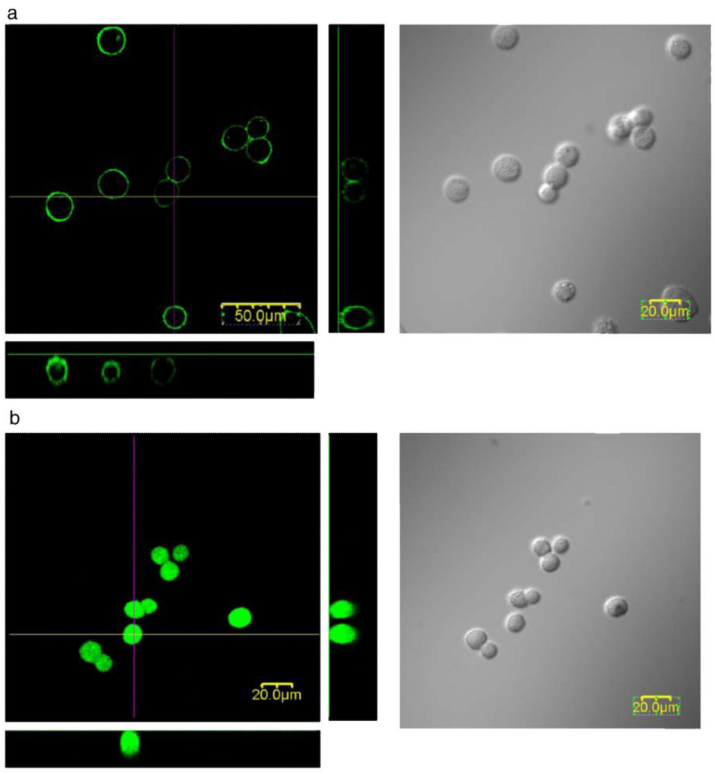

Fig. 6.

Confocal fluorescence and differential interference images of (a) FITC-PEG-lipid-modified HEK293 cells and (b) FITC-treated HEK293 cells. (a) A solution of FITC-PEG-lipid in HBSS was added to an HEK293 cell suspension ([PEG-lipids]=100 μM). (b) An aqueous solution of FITC was added to a HEK293 cell suspension. These pictures were taken within an hour after incubation with PEG-lipids for 2 h. Reproduced, with permission, from Ref. [276].

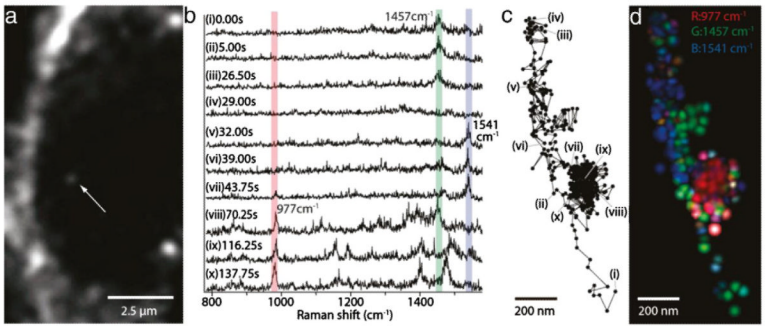

Fig. 7.

SERS analysis of the cellular pathway with an endocytosed gold nanoparticle. (a) An image of a J774A.1 macrophage cell obtained with a dark-field microscope. The white arrow indicates a gold nanoparticle, seen as a small white spot. The gold nanoparticle is taken up by endocytosis of the cell. (b) SERS spectra, obtained from the nanoparticle indicated in panel a. Characteristic Raman peaks were observed at 977 cm^{-1} (assigned to the vibration mode of phosphate), 1457 cm^{-1} (vibration mode of CH2 and CH3), and 1541 cm^{-1} (vibration mode of Amide II). These three Raman peaks are overlaid with bars in red, green, and blue. (c) Trajectory of the nanoparticle, marked by a white arrow in panel a, obtained from the dark-field images. (d) An RGB color map of the molecular distribution displayed on the nanoparticle trajectory. Green spots show the Raman intensity distribution of 1457 cm^{1}, blue spots 1541 cm^{-1}, and red spots 977 cm^{-1}. The green and blue colors are highlighted along the linear paths, while the red color appears along the confined zone random walk. The spatial resolution is determined as ~65 nm, resulting from the particle diameter of ~50 nm and a measurement accuracy of ~15 nm. Reproduced, with permission, from Ref. [296]. (For interpretation of the references to color in this figure legend, the reader is referred to the web version of this article.)

Table 1

Multimodal hybrid nanoparticles.

	Core Material	Imaging Modality (Core)	Image Material (Shell)	Imaging Modality (Shell)	Ref.	
Metal Oxides	Iron oxide	MRI	Gold	CT	[246,247,316]	
			Cy5.5	Optical	[252]	t1.5
			QD	Optical	[317]	t1.6
			^{64}Cu chelate	PET	[318]	t1.7
			$^{99\,m}$TC	SPECT	[319,320]	t1.8
	Gadolinium oxide	MRI	^{111}In	SPECT	[321]	
			Rhodamine B	Optical	[322]	t1.10
	Manganese oxide	MRI	^{125}I	SPECT	[323]	
Heavy metals	Gold	CT	Gadolinium	MRI	[255]	
			Cy5.5	Optical		t1.14
			ICG	Optical	[324]	t1.15
			Gadolinium	MRI	[325,326]	t1.16
			^{18}F	PET	[327]	t1.17
			$^{99\,m}$TC	SPECT	[328]	t1.18
Crystals	Nanophosphors	Optical (upconverted)	Iron oxide	MRI	[329]	
		Optical (upconverted), MRI	^{18}F	PET	[330]	
	Quantum dots	Optical imaging	Gadolinium chelate	MRI	[331,332]	
			Dysprosium chelate	MRI	[333]	t1.23
			^{64}Cu complex	PET	[334]	t1.24
Polymers	Perfluorocarbons	MRI, CT, USG	Europium chelate	PARACEST MRI	[248]	
	Dendrimer	Only scaffold	Gadolinium chelate	MRI	[254]	
			Cy5.5	optical		t1.28
	Block copolymer PS16-b-PAA10		Iron oxide	MRI	[335]	
			Nanophosphor	optical (upconverted)		t1.30
	Mesoporous silica		Gadolinium complexes	MRI	[249]	
			FITC	optical		t1.32
	Lipid polymer		Gadolinium complexes	MRI	[250]	
			Rhodamine	optical		t1.34

Core Material	Imaging Modality (Core)	Image Material (Shell)	Imaging Modality (Shell)	Ref.	
Polyelectrolyte		$MnFe_2O_4$	MRI	[251]	
		QD800	optical		t1.36
Chitosan		Iron oxide	MRI	[253]	
		Cy5.5	optical		t1.38